Five-fold way to new high T_c superconductors

G BASKARAN

The Institute of Mathematical Sciences, C.I.T. Campus, Taramani, Chennai 600 113, India
E-mail: baskaran@imsc.res.in

Abstract. Discovery of high T_c superconductivity in $La_{2-x}Ba_xCuO_4$ by Bednorz and Muller in 1986 was a breakthrough in the 75-year long search for new superconductors. Since then new high T_c superconductors, not involving copper, have also been discovered. Superconductivity in cuprates also inspired resonating valence bond (RVB) mechanism of superconductivity. In turn, RVB theory provided a new hope for finding new super-conductors through a novel electronic mechanism. This article first reviews an electron correlation-based RVB mechanism and our own application of these ideas to some new noncuprate superconducting families. In the process we abstract, using available phe-nomenology and RVB theory, that there are five directions to search for new high T_c superconductors. We call them five-fold way. As the paths are reasonably exclusive and well-defined, they provide more guided opportunities, than before, for discovering new superconductors. The five-fold ways are (i) copper route, (ii) pressure route, (iii) diamond route, (iv) graphene route and (v) double RVB route. Copper route is the doped spin-$\frac{1}{2}$ Mott insulator route. In this route one synthesizes new spin-$\frac{1}{2}$ Mott insulators and dopes them chemically. In pressure route, doping is not external, but internal, a (chemical or ex-ternal) pressure-induced self-doping suggested by organic ET-salts. In the diamond route we are inspired by superconductivity in boron-doped diamond and our theory. Here one creates impurity band Mott insulators in a band insulator template that enables super-conductivity. Graphene route follows from our recent suggestion of superconductivity in doped graphene, a two-dimensional broadband metal with moderate electron correlations, compared to cuprates. Double RVB route follows from our recent theory of doped spin-1 Mott insulator for superconductivity in iron pnictide family.

Keywords. High T_c superconductivity; resonating valence bond theory; cuprates; organics; boron-doped diamond; graphene; Fe pnictide superconductors.

PACS Nos   **74.72.-h; 74.20.-z; 74.10.+v; 74.62.-c**

0. Introduction

Ever since superconductivity was discovered by Kammerling-Onnes in 1911, there has been continuing efforts to find new superconductors with higher transition tem-peratures. Decades of efforts and rather slow progress culminated in the discovery of high T_c superconductivity in $La_{2-x}Ba_xCuO_4$ by Bednorz and Muller [1] in 1986. This discovery opened the flood gate and new members of cuprate family were synthesized, one of them reaching a $T_c \sim 163$ K under pressure. Finding supercon-ductivity in layered cuprates, a ceramic, was a key event from material science and

basic science point of view. It gave confidence and intensified efforts to find newer superconductors. From basic science point of view, a $T_c \sim 163$ K in a Tl-based cuprate, six times larger than the previous world record of $T_c \sim 23$ K in Nb_3Ge shook the foundation of phonon-mediated pairing mechanism. In fact, certain internal constraints arising from the stability of ordinary solid puts a restriction [2] on electron–phonon mechanism reaching a T_c beyond about 30 K. Phonon mechanism which has worked so well in elemental metals is clearly not applicable. Anderson's resonating valence bond mechanism of superconductivity, an electronic mechanism based on doped spin-$\frac{1}{2}$ Mott insulator was born [3].

It is an interesting historical fact that Bednorz and Muller were inspired by an electron–phonon mechanism of superconductivity based on Jahn–Teller bipolarons [4], that questioned the above limits on T_c. The discovery of high superconductivity in $La_{2-x}Ba_xCuO_4$ family is serendipitous, as there is no Jahn–Teller effect in $La_{2-x}Ba_xCuO_4$, but a novel electron correlation mechanism of high T_c superconductivity that was soon enunciated by Anderson and coworkers. It is this electron correlation mechanism that we will focus on in this paper.

Since 1986 many new superconducting compounds have been synthesized. Some of them are similar to cuprates, some are not, some are striking and some are less striking. In the last two decades I have looked at many of them and have suggested [5–8] non-phononic mechanism of superconductivity. In the process it has become clear that some of the systems indeed point to a new road to synthesize new superconductors. This has been pointed out by me in the context of organic superconductors and boron-doped diamond superconductor [5,6]. The aim of the present article is to look at most of the known new superconductors looking for suggestions for new routes to high-temperature superconductivity. I find that there are about five reasonably distinct routes to high-temperature superconductivity, which I call the five-fold way (figure 1). Basic to all routes are electron correlations, both weak and strong.

This paper will introduce and elaborate on the five-fold way to high T_c superconductivity. The five ways are: (i) copper route, (ii) pressure route, (iii) diamond route, (iv) graphene route and (v) double RVB route. This paper is divided into nine major sections. In §1, we will give an introduction to electron correlation-based mechanism of superconductivity, that is at the heart of resonating valence bond (RVB) theory. This section will be a pedagogic introduction to RVB theory of superconductivity. Section 2 will discuss the copper route, where one focusses on doped spin-$\frac{1}{2}$ Mott insulators. Section 3 will discuss a route suggested by organic superconductors, called pressure route. Here, within a family of the organic ET-salts [9,10], there are some members which are spin-$\frac{1}{2}$ Mott insulators and others the superconductors. One can go between the Mott insulating state and superconducting phase, at low temperatures, using either physical or chemical pressure. We have called this pressure-driven superconducting state to arise from self-doping of the Mott insulator. That is, the metallic side of the Mott transition point is viewed as a Mott insulator that has self-consistently generated an equal density of electrons and holes. Instead of an external doping one has an internal doping or self-doping.

Section 4 is called the 'diamond route'. The genesis of this route is the discovery of superconductivity in boron-doped diamond [11–13], and our theory [6]
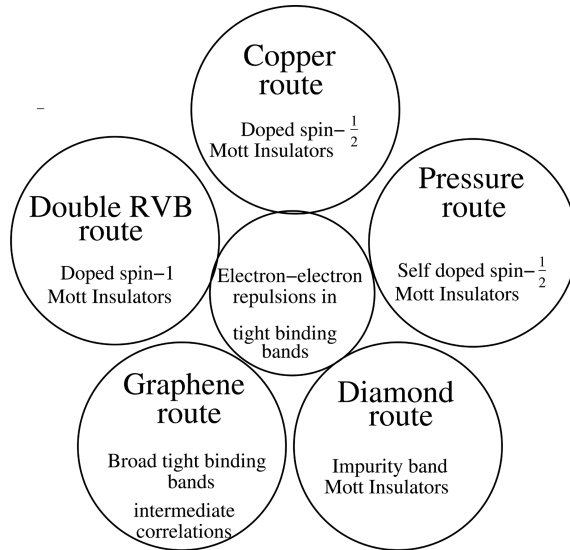
Figure 1. Five different paths to synthesize new high temperature supercon-
ductors using singlet induced by electron–electron repulsion in a tight binding
model as a basic mechanism.

based on the notion of 'impurity band Mott insulator'. Here, in a band insulator
template, dopant impurity states create narrow impurity bands; strong electron
correlations within the impurity band establishes superconductivity similar to or-
ganics. In §5, called 'graphene route', we summarize our recent findings [7] of the
possibility of high T_c superconductivity in an intermediate or less strongly corre-
lated two-dimensional electronic system, namely doped graphene. Our finding for
graphene suggests a new graphene route. Section 6 explains about the 'double
RVB route'. This route was inspired by the recent finding of a new family of Fe
pnictide superconductors [14,15]. This fascinating system has a striking similarity
to cuprate phase diagram. I have developed a theory [8] called double RVB theory
to describe superconductivity in this system. Our theory automatically suggests
a spin-1 route to superconductivity, which we call the iron route or double RVB
route. Some discussions about open problems are presented in §8. Some concluding
remarks are made in §9.

Earlier suggestions for room temperature superconductivity come from (i) Little
[16] and Ginzburg [17], where phonons which mediates attractive interactions is
replaced by a high energy exciton of the polarizable medium, (ii) bipolaron route
and (iii) metallic hydrogen (obtainable at ultra-high pressures), with a very high
Debye frequency. Unfortunately, these suggestions have not materialized so for. In
§7 we discuss other routes briefly.

The five routes that we are suggesting is a synthesis of what we have learned over
the last 20 years from cuprates onwards. Condensed matter systems being rich and
complex, many routes for high T_c superconductivity should be tried. Theory and
physical insights can be good guidelines. The richness of quantum condensed matter
physics does not seem to fail experimental colleagues who try hard. Two well-known

examples are: (i) a careful search for Wigner crystal in quasi-two-dimensional electron gas in the presence of strong magnetic field lead to the fascinating integer and fractional quantum Hall states and (ii) it was a search for Jahn–Teller bipolaron superconductivity that lead to a new route of electron correlation-based superconductivity. Our electron correlation-based theory being robust from physics and phenomenology point of view, one might in addition to high T_c superconductivity, discover some novel quantum states.

1. Introduction to RVB theory of superconductivity

The idea of resonating valence bond states arose originally in the context of $p\pi$ bonded systems, such as benzene, anthracene, naphthalene etc. by Pauling [18] and collaborators. Pauling also used it to describe some properties of semi-metallic graphite and also several metals. In 1973, Anderson suggested [19] that a natural place for resonating valence bond states are spin-$\frac{1}{2}$ Mott insulators, in the presence of large quantum fluctuations. Lower dimensionality and geometrical frustrations can encourage such quantum fluctuations. It is interesting that Anderson's article was partly a reaction to Pauling's overuse of RVB ideas in metals, even at the expense of experimentally proved notion such as Fermi surface. With the discovery of superconductivity in $La_{2-x}Ba_xCuO_4$ by Bednorz and Muller, Anderson realized that the resonating valence bond states are very special in the sense that they turn into high-temperature superconducting state on doping. While the initial focus was on superconductivity, it was very soon realized that the metallic normal state of such superconductors are very special and differ from conventional metals that are well-described by Fermi liquid theory. So resonating valence bond states got elevated to the level of a non-Fermi liquid state with anomalous normal metallic phase and also exotic broken symmetry states at low temperatures.

In the present article we will focus on RVB states from superconductivity point of view only. As Mott insulators are seats of high-temperature superconductivity, we will start with a discussion of Mott insulators. Further, La_2CuO_4, the parent cuprate compound, has turned out to be an excellent two-dimensional spin-$\frac{1}{2}$ Mott insulator. We will direct our Mott insulator and doped Mott insulator discussion through La_2CuO_4.

1.1 *Mott insulator and Hubbard model*

La_2CuO_4 is a layered perovskite: corner sharing CuO_6 octahedral form a 2D square lattice [1]. These layers are stacked along the c-axis, with intervening La atoms. Planar structure and quantum chemistry, rather than Jahn–Teller effect, is the primary cause for an elongated octahedra. The octahedra are distorted and has an elongation along the c-axis. The nominal valence of La_2CuO_4 is $La_2^{3+}Cu^{2+}O_4^{2-}$. While La^{3+} and O^{2-} have filled shells, Cu^{2+} has the unfilled shell configuration $3d^9$. Crystal field and covalency effects isolate out one Wannier orbital around Cu atom having the symmetry $3d_{x^2-y^2}$. This orbital is a symmetry adapted hybrid of copper $3d_{x^2-y^2}$ and the 2p orbitals of four neighbouring oxygen atoms. The

Wannier orbitals overlap and form a simple tight binding band. The hopping matrix element $t_\perp$ is small ($\frac{t}{t_\perp} \ll 1$) along the c-axis, resulting in electronic isolation of the CuO_2 layers along the c-axis. Thus the kinetic energy part of the Hamiltonian is given by

$$H_0 = -\sum_{ij} t_{ij} c_{i\sigma}^\dagger c_{j\sigma} + \text{h.c.} = \sum_k \epsilon_{\mathbf{k}} c_{\mathbf{k}\sigma}^\dagger c_{\mathbf{k}\sigma}. \tag{1.1}$$

Here the site index refers to a Wannier orbital and $\mathbf{k}$ are the two-dimensional wave vectors defined inside the square lattice Brillouin zone. The two-dimensional tight binding model leads to a narrow band, characteristic of 3d transition metal oxides, of width ∼3 eV.

The band is half-filled and is expected to be a metal. In reality La_2CuO_4 is insulating and challenges the simple band picture. The insulating character follows from the fact that the filling is commensurate (an average occupancy of 1 electron per Wannier orbital) and that on-site Coulomb repulsion U is larger than the bandwidth and prevents Bloch state formation and Fermi surface formation. In other words, it is energetically favourable for each site to have one localized electron. This is Mott localization, where each electron looses kinetic or delocalization energy ($\approx$ bandwidth) but gains the repulsion energy U per site, by avoiding close encounters such as a doubly occupied singlet site. The physics of Mott insulator is well captured by the repulsive Hubbard model:

$$H = -t \sum_{\langle ij \rangle} c_{i\sigma}^\dagger c_{j\sigma} + \text{h.c.} + U \sum_i n_{i\uparrow} n_{i\downarrow}. \tag{1.2}$$

This model, though simple looking, has turned out to be one of the richest models in terms of physics content and also challenging from quantitative many-body theory point of view. In one dimension, Lieb and Wu [20] have solved this problem, for arbitrary fillings, for wave functions and energy eigenvalues, through Bethe ansatz solution. In two dimensions, no exact solutions exist. However, a good qualitative and sometimes quantitative understanding exist, thanks to the efforts that started with RVB theory of cuprates.

1.2 *Spin states of Mott insulators*

Mott insulator, unlike a band insulator, has low energy, often gapless spin carrying excitations. Charge carrying excitations have a finite energy gap. This is a kind of spin-charge decoupling: spin excitations are soft and charge excitations are hard (figure 2). Further, spins tend to have long-range order, because of superexchange interaction. The case of interest to us is RVB states, a disordered spin state or a spin liquid phase which arises from strong quantum fluctuations.

It is customary to start from the large $U \gg t$ limit and derive effective spin Hamiltonian in powers of t/U. This is called superexchange perturbation theory or hopping parameter expansion. In the atomic limit, $t = 0$, a highly degenerate set of ground states of the Hubbard model at half filling is given by
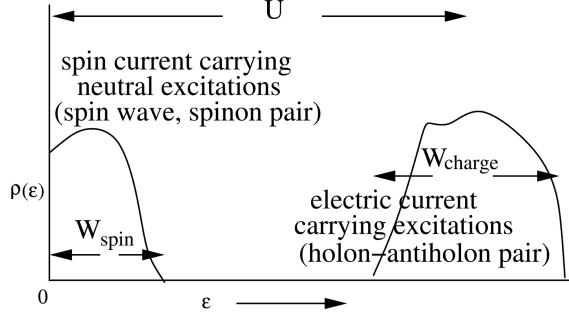
Figure 2. Schematic density of states of spin current carrying excitations and charge current carrying excitations. W_{spin} and W_{charge} are bandwidths of the neutral and electrical current excitations.

$$|\sigma_1, \sigma_2, ..., \sigma_N\rangle \sim \prod_{i=1 \text{ to } N} c^\dagger_{i\sigma_i}|0\rangle. \tag{1.3}$$

In these states, every site is singly occupied and has a dangling spin. Consequently, total spin degeneracy of this manifold is 2^N. The extensive spin entropy of the above states are removed by superexchange, a second-order hopping process, involving two neighbouring sites at a time. By a second-order perturbation procedure we can derive an effective Hamiltonian that lifts the 2^N-fold spin degeneracy. For a given pair of neighbouring sites, the four ground states in the atomic limit are: (i) a bond singlet state $\frac{1}{\sqrt{2}}(|\uparrow,\downarrow\rangle - |\downarrow,\uparrow\rangle)$ and (ii) three bond triplets $|\uparrow,\uparrow\rangle$, $|\downarrow,\downarrow\rangle$, $\frac{1}{\sqrt{2}}(|\uparrow,\downarrow\rangle + |\downarrow,\uparrow\rangle)$ of two spins of neighbouring sites. When hopping t is introduced perturbatively, there is a virtual transition or mixing of the singlet state with the excited 'ionic spin singlet' intermediate configurations:

$$\frac{|\uparrow,\downarrow\rangle - |\downarrow,\uparrow\rangle}{\sqrt{2}} \quad \rightarrow \quad \frac{|\uparrow\downarrow,0\rangle + |0,\uparrow\downarrow\rangle}{\sqrt{2}} \quad \rightarrow \quad \frac{|\uparrow,\downarrow\rangle - |\downarrow,\uparrow\rangle}{\sqrt{2}}$$

resulting in an energy gain $J = 4t^2/U$, for the bond singlet ground state. As far as the triplet states are concerned they cannot undergo a virtual transition to an intermediate ionic configuration, because of Pauli blocking. Thus, triplet states do not gain energy through the kinetic process. The different ways in which bond singlet and bond triplet states get affected appears as an effective antiferromagnetic Heisenberg Hamiltonian, defined in the 2^N-dimensional Hilbert space of the low energy spin degrees of freedom of the Mott insulator:

$$H(\text{half filling}) \rightarrow H_s = J \sum_{\langle ij \rangle} \left(\mathbf{S}_i \cdot \mathbf{S}_j - \frac{1}{4} \right), \tag{1.4}$$

where $J = 4t^2/U$.

Before the advent of RVB theory, disordered spin states in Mott insulators were always associated with high temperature phases, where thermal fluctuations have destroyed a long-range magnetic order. There is no special quantum coherence associated with these disordered spin states, except perhaps some short-range order
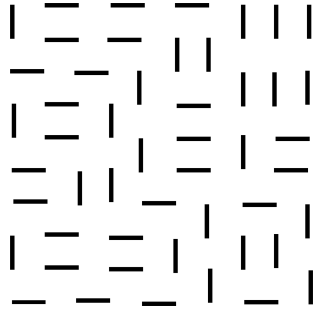
Figure 3. One of the bond configurations of a short-range RVB state.

and related dynamics. Anderson [19] suggested in 1971 that there can be a genuine zero temperature nondegenerate disordered spin state, a quantum liquid of spins having special quantum coherence properties. In particular, he suggested simple RVB state to represent such a quantum spin liquid state and applied it to the study of ground state of spin-$\frac{1}{2}$ Heisenberg antiferromagnet in triangular lattice in two dimensions. It turned out to be a straightforward generalization of Pauling's RVB states to a triangular lattice.

The conjecture of Anderson that the spin liquid ground state will in general be nondegenerate is to do with the fact that maximum phase coherence among difference valence bond configurations implies a coherent delocalization of valence bond and hence maximization of resonance energy.

To make connection with cuprates, we will discuss a simple short-range RVB state for a square lattice, suggested by Kivelson *et al* [21], quickly following Anderson's suggestions for cuprates:

$$|\text{RVB}\rangle \equiv \sum_C |C\rangle. \tag{1.5}$$

Here C represents a covering of the square lattice with nearest-neighbour dimers (singlet pairs) such that every spin is part of a dimer (figure 3). There are exponentially large number of such configurations. We give equal weightage to these configurations and sum over all of them with identical phase. In defining the spin function for the square lattice which has a bipartite structure we follow a sign convention to satisfy Marshall rule. A nearest-neighbour bond $\langle ij \rangle$ has a spin wave function $\frac{1}{2}(\alpha_i\beta_j - \beta_j\alpha_i)$ and we should ensure that i and j belong to sublattice A and B respectively.

The above state, as a variational state, is not good for a square lattice spin-$\frac{1}{2}$ antiferromagnetic Heisenberg model. Standard antiferromagnetically ordered state, as given by spin wave theory, gives lower energy per spin. However, by introducing slightly longer singlet bonds, one can minimize the energy further. That is, there are short-range variational RVB wave function with spin–spin correlation length of the size of few lattice parameters, whose energy is higher than the exact ground state energy only by less than a per cent.

RVB states represent a unique class of wave functions in many-body theory. They cannot be expressed as a simple Slater determinant. In a technical sense
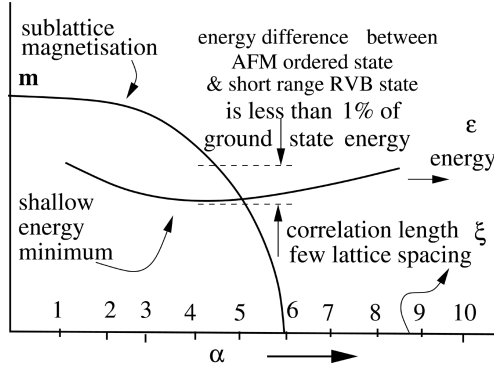
Figure 4. Schematic picture of the results of numerical analysis of Liang—Doucot–Anderson RVB wave function. This wave function exhibits spontaneous symmetry breaking as a function of parameter α, that defines the range of the valence bond. Notice that the energy of this state has a shallow minimum around $\alpha = 4$, corresponding to an AFM-ordered state with nearly 50% sublattice magnetization. The minimum energy is very close to the results found by other methods. When $\alpha \approx 9$, there is no long-range order and the AFM correlation length is few lattice parameters; however, the energy is higher than the ground state by less than a per cent.

they are strongly entangled. They may be thought of as a class of Jastrow-type of functions, however. These states accommodate singlet pair correlations right at the start, rather than filling single-particle states. We will go to the precise definition later.

An RVB variational wave function discovered by Liang *et al* [22] demonstrates this (figure 4) very well. The wave function is given as

$$|\text{RVB}, \alpha\rangle \equiv \sum_C \left[\prod_{ij(C)} \frac{1}{R_{ij}^\alpha} \right] |C\rangle. \tag{1.6}$$

This is a long-range RVB wave function that contains singlet bonds that connect any two arbitrary sites, but belonging to different sublattices. The weight of the longer bonds are reduced as a function of their length in a power law fashion. That is, a configuration C containing $N/2$ has the following weight: it is a product of $1/R_{ij}^\alpha$ over all pairs in a given configuration C. Here R_{ij} is the distance between two sites i and j.

Liang *et al* showed by extensive numerical study (figure 4) that the above RVB wave function exhibits spontaneous symmetry breaking (a two-sublattice antiferromagnetic order) for $0 < \alpha < 6$. The order parameter continuously vanishes as one reaches the critical value $\alpha \approx 6.0$. When α exceeds 6, there is no long-range order and it describes a spin liquid state with short-range antiferromagnetic order. What is remarkable is that the energy expectation value of this state for the 2D square lattice spin-$\frac{1}{2}$ Heisenberg Hamiltonian has a shallow minimum at $\alpha \approx 4$, corresponding to a minimum energy (per spin in units of J) $E = -0.544 \pm 0.0002$. When α falls well into the disordered state, the energy $E = -0.5437$, within one per

cent of the exact ground state energy. This indicates that singlet correlations are the robust part of the ground state and antiferromagnetic order is only a peripheral change, an apparent order that hides lots of inherent quantum disorder.

Because of the above, the antiferromagnetically ordered state in 2D is not robust and is very sensitive to doping of the Mott insulator and other perturbations. So it is not a good reference state to study doped Mott insulators such as $La_{2-x}Sr_xCuO_4$. This particular aspect has not been well appreciated in the literature. Several authors tend to hold onto antiferromagnetic correlations even in the optimally doped region in cuprates, where the physics is that of a quantum spin singlet fluid containing doped charges.

1.3 *RVB mean field theory*

How do we obtain resonating valence bond states in a systematic many-body theory approach? A rather unconventional many-body theory was provided by Baskaran, Zou and Anderson [23] (BZA). This approach involved enlarging the Hilbert space of the problem. We are used to enlarging the Hilbert space, for example in the Holstein–Primakoff spin wave theory, where the Hilbert space dimension of a given spin, instead of being $2S + 1$, becomes an infinite-dimensional Hilbert space of a harmonic oscillator. The Hilbert space enlargement we introduced was something natural and it enabled us to see the structure of spin liquid state and nontrivial possibilities in a more transparent fashion. This method has turned out to be well suited to study general quantum spin liquid states. An excellent recent example is the exactly solvable Kitaev model [24], a spin-$\frac{1}{2}$ model defined on a honeycomb lattice. We have shown that RVB mean field theory gives exact results [25] for the same model.

We rewrite the Heisenberg model in terms of the underlying electron operators:

$$H_s = J \sum_{\langle ij \rangle} \left(\mathbf{S}_i \cdot \mathbf{S}_j - \frac{1}{4} \right) = -J \sum_{\langle ij \rangle} b_{ij}^\dagger b_{ij} \tag{1.7}$$

using the relation, $\mathbf{S}_i \equiv \sum_{\alpha,\beta} c_{i\alpha}^\dagger \vec{\tau}_{\alpha\beta} c_{i\beta}$, where $\vec{\tau}$ is the Pauli spin operator and c's are the electron operators that constitute the physical magnetic moment. Further, $b_{ij}^\dagger \equiv \frac{1}{\sqrt{2}}(c_{i\uparrow}^\dagger c_{j\downarrow}^\dagger - c_{i\downarrow}^\dagger c_{j\uparrow}^\dagger)$ is the bond singlet or (in the present case) neutral Cooper pair operator. In the electron representation the Heisenberg Hamiltonian has a simple meaning. The spin–spin coupling encourages bond singlets, because it is minus of the bond singlet number operator $b_{ij}^\dagger b_{ij}$. The nontrivial character of the lattice problem arises from the fact that the bond singlet number operators do not commute, if they share one common site. In [26], recently a very useful commutation relation was showed:

$$[b_{ij}^\dagger b_{ij}, b_{jk}^\dagger b_{jk}] = \mathbf{S}_i \cdot (\mathbf{S}_j \times \mathbf{S}_k). \tag{1.8}$$

This relation defines spin current related to delocalization of singlet pairs. Such spin current turns out to be the local spin chirality $\mathbf{S}_i \cdot (\mathbf{S}_j \times \mathbf{S}_k)$.

Let us look at the nature of the problem in the enlarged Hilbert space whose dimension is 4^N, as opposed to 2^N dimensions of the spin space. The Hamiltonian

acquires some local symmetry in the enlarged Hilbert space [27,28]. What is remarkable is that the structure of the Hamiltonian in terms of the slave particle variable is well-suited to describe quantum spin liquid state that can support quantum number fractionization. That is, the spin-1 (Goldstone mode) excitation of an ordered antiferromagnet can break into two spin-half spinon excitations in an RVB state. A spinon operator has no simple form in terms of the original spin variable, whereas it becomes simple in terms of the constituent electron operator.

Even though the form of the Hamiltonian in the enlarged Hilbert space is suggestive of RVB physics it is still not exactly solvable in the electron representation. It is a problem of electrons interacting with nearest-neighbour attraction in spin singlet channel in a half-filled band of zero bandwidth (absence of kinetic energy). So it suggests Cooper pairing phenomena among spins and possibility of a simple Bogoliubov–Hartree–Fock-type approximation.

A practical way to get approximate eigenfunctions in the physical Hilbert space is to project our mean field solutions to physical Hilbert space. The resulting state will be the approximate eigenfunctions of our original problem.

We will use the similarity of our problem to BCS Hamiltonian and solve it approximately. In k-space the Cooper pair scattering term arising from superexchange has the following form:

$$H_{\text{pair}} = -J \sum_{k,k'} \gamma(\mathbf{k} - \mathbf{k}') c^\dagger_{-k'\downarrow} c^\dagger_{k'\uparrow} c_{k\uparrow} c_{-k\downarrow} \tag{1.9}$$

with the pair potential having the form, $\gamma(\mathbf{k} - \mathbf{k}') \sim [\cos(k_x - k'_x) + \cos(k_y - k'_y)]$. It should be noted that the pair potential, while it is attractive for small momentum transfer $(\mathbf{k} - \mathbf{k}') \sim 0$, changes sign and becomes repulsive for large momentum transfer $\sim (\pi, \pi)$, manifestly suggesting a $d_{x^2-y^2}$-wave rather than extended-s wave as a low energy mean field solution. The BZA mean field solution however, focussed on extended-s rather than d-wave mean field solution. Later works by Affleck–Marston [29], Kotliar [30] and Gros–Joynt–Rice [31] brought out d-wave mean field solution.

In our Bogoliubov–Hartree–Fock factorization we have the self-consistant parameters:

$$\Delta \equiv \sum_k (\cos k_x + \cos k_y) \langle c^\dagger_{k\uparrow} c^\dagger_{-k\downarrow} \rangle$$

and

$$p \equiv \sum_{k\sigma} (\cos k_x + \cos k_y) \langle c^\dagger_{k\sigma} c_{k\sigma} \rangle. \tag{1.10}$$

The first one Δ is the usual anomalous superconducting amplitude. The second one p is somewhat unconventional, it is a kinetic energy or hopping term, a 'Hartree–Fock vector potential', generated by superexchange process. This unusual Hartree–Fock factorization term introduced in this paper played crucial role in later developments, such as gauge theory [27] and Affleck–Marston's flux phase [29]. The simplest self-consistent solution was found to be $\Delta = 1$ and $p = 0$. After the Bogoliubov transformation we find the following quasi-particle Hamiltonian for gapless spinon excitations, α's:

$$H_{\mathrm{mF}} \sim J \sum_{k\alpha} |\cos k_x + \cos k_y| \alpha_{k\sigma}^\dagger \alpha_{k\sigma}. \tag{1.11}$$

What is remarkable is that the absence of kinetic energy results in a Fermi surface for the spinons given by the expression $|\cos k_x + \cos k_y| = 0$. Further, the anomalous pairing leads to a remarkable result for the ground state occupancy

$$n_{k\sigma} \equiv \langle c_{k\sigma}^\dagger c_{k\sigma} \rangle = 1. \tag{1.12}$$

Even though neutral fermion excitations have a pseudo-Fermi surface, there is no momentum space discontinuity for the constituent electrons. In this sense this spin liquid ground state of the Mott insulator is far removed from any standard Fermi liquid state. The ground state as given by our theory in the enlarged Hilbert space is a BCS wave function (mean field RVB wave function):

$$|\mathrm{RVBmF}\rangle = \prod_k (u_k + v_k c_{k\uparrow}^\dagger c_{-k\downarrow}^\dagger)|0\rangle \tag{1.13}$$

with $(v_k/u_k) = \pm 1$ inside and outside the pseudo-Fermi surface respectively. The N particle projected BCS wave function has a suggestive form of RVB state:

$$|\mathrm{RVBmF}\rangle = \left(\sum \phi_{ij} b_{ij}^\dagger \right)^{N/2} |0\rangle. \tag{1.14}$$

Here the Cooper pair function ϕ_{ij} is the Fourier transform of the ratio u_k/v_k. It is an oscillatory function that decays in a power-law fashion. This real space picture tells us that $N/2$ singlet pairs are Bose condensed into a zero momentum state. The singlets are not just nearest-neighbour pairs but have an amplitude given by ϕ_{ij} for a separation ij.

We obtain our approximate wave function in the physical Hilbert space by Gutzwiller projecting our mean-field RVB state to singly occupied states:

$$|\mathrm{RVB}\rangle = P_{\mathrm{G}} \prod_k (u_k + v_k c_{k\uparrow}^\dagger c_{-k\downarrow}^\dagger)|0\rangle$$

$$= P_{\mathrm{G}} \left(\sum \phi_{ij} b_{ij}^\dagger \right)^{N/2} |0\rangle. \tag{1.15}$$

Here $P_{\mathrm{G}} \equiv \prod_i (1 - n_{i\uparrow} n_{i\downarrow})$ removes any double occupancy and ensures single occupancy at every site. Equation (1.15) also defines a general resonating valence bond state for an arbitrary choice of the function ϕ_{ij}. By choosing $\phi_{ij} = \pm 1$ for nearest-neighbour bonds along the x and y directions respectively and zero otherwise, we reproduce the short-range RVB wave function (eq. (1.5)).

1.4 *Doped Mott insulators*

The Heisenberg Hamiltonian captures the physics of low energy spin degrees of freedom of the Mott insulator. Once we introduce carriers into the Mott insulator, through doping of holes in $\mathrm{La_{2-x}Sr_xCuO_4}$ for example, we have charge delocalization through hole dynamics. That is, the Mott insulating character is disturbed

and low energy charge degree of freedom are introduced to the extent of external doping. Further, superexchange survives among the correlated electrons for a finite range of doping. This is summarized in an effective Hamiltonian called t-J model, that became extremely popular after the RVB theory of cuprate superconductivity. We will not discuss the derivation of this Hamiltonian; in the context of cuprates, this single band model also needs further analysis *à la* Zhang–Rice singlet [32] formation. This model contains kinetic energy or hopping term for holes in addition to the Heisenberg coupling among the spins:

$$
\begin{aligned}
H_{\mathrm{tJ}} &= H_t + H_s \\
&= -\sum_{\langle ij \rangle} t_{ij} c_{i\sigma}^{\dagger} c_{j\sigma} + \mathrm{h.c.} + J \sum_{\langle ij \rangle} \left(\mathbf{S}_i \cdot \mathbf{S}_j - \frac{1}{4} n_i n_j \right)
\end{aligned}
\tag{1.16}
$$

with a double occupancy constraint, $n_{i\uparrow} + n_{i\downarrow} \neq 2$ at every site. Cuprates have a large superexchange $J \sim 0.15$ eV, one of the largest among spin-$\frac{1}{2}$ Mott insulators.

The BZA theory, which suggested an RVB mean field theory for the Mott insulator also provided a mean field theory for doped Mott insulators. This theory undertook this variational analysis. This is similar to a BCS-Hartree–Fock-type analysis, but in a restricted Hilbert space containing no double occupancy. That is, one would like to minimize the energy expectation value (or free energy) with respect to the pair function $\phi(ij)$:

$$
E[\phi] = \langle \mathrm{RVBmF}; \phi | P_{\mathrm{G}} (H_t + H_s) P_{\mathrm{G}} | \mathrm{RVBmF}; \phi \rangle.
\tag{1.17}
$$

The presence of Gutzwiller projector P_{G} makes analytical calculations rather difficult. So this theory introduced a physically motivated approximation. The approximation amounts to treating the Gutzwiller projection in a mean field fashion and approximate the above expression by

$$
E[\phi] \approx \langle \mathrm{RVBmF}; \phi | (x H_t + H_s) | \mathrm{RVBmF}; \phi \rangle.
\tag{1.18}
$$

That is, the complicated Gutzwiller projection was approximated by replacing the hopping parameter t by a renormalized parameter xt, since x is the probability that an electron can find a neighbouring site empty to which it can hop. In other words, we have a renormalized Hamiltonian

$$
\tilde{H}_{\mathrm{tJ}} = x H_t + H_s
\tag{1.19}
$$

defined in the full Hilbert space, also containing double occupancies. The rest is very similar to standard BCS theory. Interestingly, this paper conjectured that this renormalization prescription should work well beyond about 5% doping, about which we will discuss later.

Within the above-mentioned approximation this theory found (i) a spin liquid ground state, neutral fermion excitations with a pseudo-Fermi surface for the Mott insulator and (ii) a superconducting ground state with extended-s symmetry for doped Mott insulator.

A mean field analysis of the renormalized Hamiltonian (eq. (1.19)) is straightforward and it gave us a BCS-type of wave function:

$$|\text{RVB}; \phi\rangle = P_G \prod_k (u_k + v_k c_{k\uparrow}^\dagger c_{-k\downarrow}^\dagger)|0\rangle$$

$$\equiv P_G [\sum_{ij} \phi(ij) b_{ij}^\dagger]^{\frac{N(1-x)}{2}}|0\rangle. \tag{1.20}$$

We can also carry on the RVB mean field theory at finite temperatures. We get a finite temperature phase transition at a transition temperature T^* even for the Mott insulator. Earlier RVB mean field theory and later developments provide an estimate of T^* as follows:

$$k_B T^* \sim J_{\text{eff}} e^{-\frac{1}{\rho_0 J_{\text{eff}}}} \sim J(1 - \alpha x), \tag{1.21}$$

where the density of states at the Fermi energy of the spinon Fermi surface $\rho_0 \approx 1/J_{\text{eff}}$ and the effective interaction among spinons is $J_{\text{eff}} \approx J(1 - \alpha x)$, where $\alpha \approx W/J$. This finite temperature phase transition is an artifact of the mean field theory. However, it has an artifact message. It can be shown [27] that because of gauge field fluctuations this mean field transition will turn into a cross-over temperature scale. It provides the scale at which spins start getting paired into singlets. This temperature indicates the beginning of the preformed neutral singlet pair formation. This was a clear prediction of RVB theory. Later experimental discovery of spin gap phenomenon in experiments is a consequence of our spin pairing phenomenon. Further, as we dope the system, the effective J gets renormalized to $J(1 - \alpha x)$, by dilution of superexchange due to doped holes. This roughly explains the linear dependence of the spin-gap temperature T^* as a function of doping x, as seen in NMR experiments for example.

What is the best we can do in terms of understanding the spin and charge behaviour of our doped Mott insulator and also superconductivity within RVB mean field theory? It turns out that we can learn a lot and even make quantitative prediction from this simple RVB mean field theory, provided we interpret the physics of what is going on properly.

In the Mott insulator the system was filled with singlet pairs. The singlets could not delocalize and produce a superconducting state, because the system was incompressible as far as the charge excitations are concerned. Now we have a fraction x of holes. To this extent the system becomes compressible. Now the pair function $\phi(ij)$ gets self-consistently modified. The original BZA solution had superconductivity with an extended-S symmetry. Soon a lower energy superconducting spin singlet state with $d_{x^2-y^2}$ symmetry with a nodal quasi-particle excitation was found. We will not discuss these issues further but directly go to simple ways of extracting superconducting transition temperatures.

How do we determine the superconducting T_c? We have to go back to our wave function and find out what is going on to determine the actual superconducting T_c. That is, by an analysis of the structure of our variational wave function we can predict superconducting T_c!

Formally, after Gutzwiller projection what we have is a small density x of holes which are delocalized in the background of neutral spin singlets. If the superconducting order parameter is nodeless we will have a short-range singlet bond. If they have a node there will be a small power-law tail, which will make a long-range RVB. What is important is that charge fluctuations arise purely because of the

presence of a density of x holes, rather than free fluctuations of singlet pairs. This is what makes the superfluid fraction in cuprates at low doping proportional to x and independent of the gap magnitude.

The original proposal of Anderson and also what followed from the BZA mean field solution was that a fraction $x\frac{N}{2}$ of spin singlet pairs got charged and are available for superconductivity. These are the Cooper pairs that interact through screened Coulomb interaction and undergo essentially Bose condensation (or Kosterlitz–Thouless order in 2D) and contribute to superfluid fraction. The background spins have been mostly silenced because of pairing. This is how a small density of Cooper pairs emerge in a doped Mott insulator.

As the notion of charged singlets is key to high T_c in RVB mechanism, we will elaborate on this. In the case of the Mott insulator all electrons are paired and the valence bonds fill the lattice and they form a charge incompressible quantum liquid. That is, there are no low energy charge degree of freedom that are available as low energy excitations. The only fluctuations available in the ground state and at low energy states are the valence bond delocalization or equivalently spin fluctuations. That is, low energy charge transport is completely absent. We need to be able to transport electron pairs across the sample, to create a superconducting state. Doping essentially makes the charge compressibility of valence bond liquid finite, thereby facilitating the formation of a coherent superconducting state.

Within the above approach, in our quasi-2D problem, the superconducting T_c is the Kosterlitz–Thouless transition temperature of a density x of charged Cooper pairs with an effective mass m_c:

$$k_B T_c \sim \frac{2\pi\hbar^2}{m_c}(x - x_c). \tag{1.22}$$

Here x_c is some critical doping needed to overcome disorder effects and begin superconductivity. The above expression has turned out to be an excellent description of superconducting T_c in doped cuprates below optimal doping. Above optimal doping the above T_c is cut off by the spin gap scale T^*; we will not go into details of this region. Below optimal doping the only way interaction parameter appears is through mass of the charged Cooper pair m_c, which encodes the bandwidth of the delocalized holes. Factors such as disorder, unscreened short-range Coulomb interactions and electron–lattice coupling will affect the charge Cooper pair mass to varying degrees, thereby changing the superconducting T_c.

The power of RVB theory is to bring out such a simple and non-BCS like x dependence of T_c, which is in agreement with experiments.

At very high doping, Mott insulator turns into a (disturbed) Fermi sea. Super-exchange becomes less relevant, as electrons are less localized because of decreasing correlations. BZA mean field theory showed a sharp decrease of the mean field T_c beyond an optimal doping. Synthesizing various ideas and the BZA mean field solutions, a phase diagram was suggested shortly [33]. This phase diagram, shown in figure 5, was also a prediction of BZA theory. The experimental phase diagram that was established later over years has a striking resemblance to this prediction.

Kivelson *et al* [21] formulated the physics of charged Cooper pair condensation of RVB theory as a Bose condensation of a density x of the novel quasi-particles, charge $+ e$ holons. This gave a feeling that one will have charge e Bose condensation. However, it was argued by us [33] that holons are only bookkeeping devices
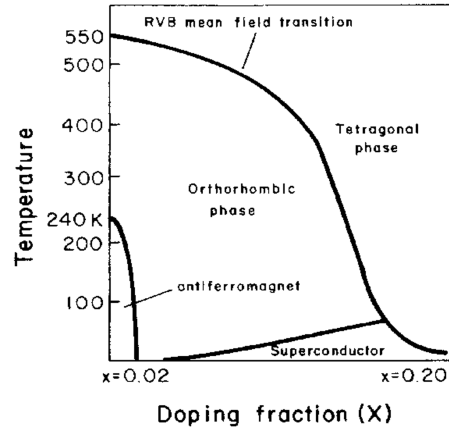
Figure 5. Schematic phase diagram of RVB theory reproduced from ref. [33]. The superconducting dome was a prediction of RVB theory in early 1987, well before it was experimentally found.

for charge $2e$ Cooper pairs that actually delocalize, proving we have charge $2e$ superconductivity phenomenon.

2. Copper route

In the previous sections we discussed how superconductivity arises in doped spin-$\frac{1}{2}$ Mott insulators. Bednorz and Muller's discovery clearly showed a route. We will call this Cooper route. The basic idea is to look for orbitally nondegenerate spin-$\frac{1}{2}$ Mott insulators and dope them externally. Surprisingly, there are not many spin-$\frac{1}{2}$ Mott insulators which have been doped. We will discuss about the nature of this route and possible difficulties one will encounter.

After the discovery of Bednorz and Muller, dozens of cuprates have been synthesized. A detailed look at them reveal that they are all doped Mott insulators. In some systems we may not be able to synthesize the parent Mott insulator, for crystal chemistry and structural reasons. What is common among all of them is the presence of CuO_2 planes and charge reservoirs outside the plane. No wonder, the new planar cuprates have followed the copper route!

We can also learn from the cuprate family, about hurdles along this route. It is a well-known fact that at optimal doping the superconducting T_c varies widely between 5 and 163 K, within the cuprate family. We have argued [34] that this variation arises because of differing competing orders. Different structures have varying tendency for strong and fluctuating lattice distortions; they in turn encourage competing orders to different degrees. That is, a strong bare electron–lattice coupling under some conditions can favour competing orders such as charge and spin localizations. Such a charge or spin localization will automatically prevent valence bond delocalization thereby decrease superconducting T_c.

In this search for new superconductors in the copper route, we have to keep in mind phenomena that compete with superconductivity. Two major competitors

are spin-Peierls state formation and Jahn–Teller distortion and dopant localization into polarons. In the spin-Peierls-type situation singlet bonds order spatially in one-dimensional structure of more complicated three-dimensional structures. This cooperative localization, which is favoured by specific structures, is often aided by the ability to undergo structural distortions. If such a distortion is already present in the Mott insulator, doping has to remove this cooperative distortion and enable valence bond delocalization.

It is interesting that many known spin-$\frac{1}{2}$ Mott insulators such as VO_2, Ti_2O_3, TiOCl, which are potential high-temperature superconductors on doping, actually undergo very high-temperature spin-Peierls instabilities. The nonplanar and chain line rutile structure of VO_2 easily allows dimerization. So far it has not been possible to dope the above into superconducting state.

Another major hurdle in the copper route is Jahn–Teller effect. In systems based on lower end of the 3d and 4d series we often occupy one of the degenerate t_{2g} levels. So to begin with there may be a spontaneous orbital order and cooperative Jahn–Teller distortions. On adding dopants we will disturb this cooperative order. Consequently, there will be local lattice distortions and the doped carrier is likely to become a heavy polaron. Another way of saying is that the charged valence bonds become heavy as they carry the lattice distortion with them. This will be detrimental to superconductivity.

Another major problem is the inability to insert dopant atoms into the structure. In cuprates the layered character allows for a liberal modification of the reservoir layers. This allows (i) a good control over doping and (ii) produce less electrostatic disorder on the CuO_2 planes arising from introduction of dopant atoms. A compact three-dimensional structure will prevent introduction of dopants. Layered and three-dimensional perovskites are good from this point of view. The cations are outside the octahedra and they can be easily replaced by dopant atoms, within some tolerance limit.

Some of the difficulties in this route is explained by the mineral tenorite CuO [45], the parent compound of La_2CuO_4. It is a good spin-$\frac{1}{2}$ Mott insulator: a three-dimensional system of chains of Cu^{2+} ions, square planar coordinated by O^{2-} ions. It has an antiferromagnetic order. The moments are reduced due to strong quantum fluctuations. According to RVB mean field theory, it should be as good a superconductor as YBCO system. However, experimentally it has not been possible to dope and metallize this system. A major reason for not being able to dope is the compact three-dimensional structure which prevents insertion of dopant atoms. In situations like this, one way to dope is by partial replacement of oxygen by fluorine or nitrogen, the right and left neighbours of oxygen in the periodic table. I do not know if this has been tried.

Difficulty to dope externally continues even in the large family of organic superconductors, such as Bechgaard salts, ET salts and fullerites.

It has been suggested [35] that the 'icy superconductor' $Na_xCoO_2 \cdot yH_2O$ is a case of electron-doped spin-$\frac{1}{2}$ Mott insulator. We have suggested [36] that in superconducting $Ba_{1-x}K_xBiO_3$ physics of doped Mott insulator is at work, even though popular belief is that it is a case of doped charge density wave system. This system needs to be investigated further.

In summary, copper route remains largely unexplored.

3. Pressure route

Theoretical possibility of pressure-induced RVB superconductivity in a Mott insulator appeared in the scene rather late, even though superconductivity in organic systems were suggesting this route loudly. There are three families of 'commensurate' or half-filled band tight binding systems that undergo Mott insulator (spin-Peierls or antiferromagnetic order) to superconductor transition under pressure or chemical pressure and no external doping: (i) quasi-one-dimensional $(TMTSF)X_2$, Bechgaard salt family [9], (ii) quasi-two-dimensional κ-$(BEDT\text{-}TTF)X_2$, ET-salt family [10] and (iii) three-dimensional fullerites [37,38]. For ET and Bechgaard salts, a single band repulsive Hubbard model at half-filling is known to be a right model [39,40].

Another less known example [41] is the pair of inorganic compounds $GaNb_4Se_8$ and $GaTa_4Se_8$, which are spin-$\frac{1}{2}$ Mott insulators. Abd-Elmeguid, partly inspired by our suggestion of pressure-induced superconductivity in spin-$\frac{1}{2}$ Mott insulator studied $GaNb_4Se_8$ and $GaTa_4Se_8$ under pressure and discovered superconductivity around 6 K after a pressure of few GPs.

3.1 *Strong coupling hypothesis*

A popular view about superconductivity in organics was that the metallic side of the pressure (chemical or physical) induced Mott transition point was a Fermi liquid having enhanced spin fluctuations at a characteristic antiferromagnetic wave vector and also somewhat larger effective mass for the quasi-particles. This view was partly due to the results from idealized Hubbard model, where tuning the parameter t/U results in a second-order transition, a continuous vanishing of the Mott–Hubbard gap. In reality, pressure-induced Mott transitions in oxides as well as organics were strongly first order: the charge gaps vanished discontinuously with a large jump. Often a significant volume change was involved. Further, the original proposal of Mott, which used long-range Coulomb interaction predicted first-order metal insulator transition.

It is in this context the present author proposed a 'strong coupling' hypothesis; it states that a generic Mott transition in real systems is to a (strong coupling) metallic state with superexchange. This hypothesis implies that the conducting state as a self-doped Mott insulator that has very nearly the same superexchange J as the insulator and a small fixed (conserved) density x of delocalized doubly occupied sites and same density x of empty sites are self-doped into the system. This enabled us to propose a generalized t-J model, where a fixed number N_0 of doubly occupied sites (e^-) and N_0 empty sites (e^+) hop in the background of $N - 2N_0$ singly occupied (neutral) sites that have superexchange interaction among themselves. Here N is the number of lattice sites. In determining the total number of mobile charges $2N_0$, that is the amount of self-doping, large-range Coulomb interaction plays an important role.

The mechanism of superconductivity in a self-doped Mott insulator is the same as externally doped Mott insulator. As a function of the amount of self-doping we also have disappearance of antiferromagnetic order and appearance of a superconducting

dome. Major difference is that we have no continuous control on the amount of self-doping. Across the Mott transition, self-doping starts with a critical value x_0. If x_0 is in the range of optimal doping for that Mott insulator, we will get maximum superconducting T_c. If x_0 is well beyond the optimal doping we will have no superconductivity.

It should be pointed out that, 1d Mott transition and various Hubbard model-based theories exist in the literature [39,40,42] for the Bechgaard, ET salts and fullerites. Our viewpoint emerging from 'strong coupling' hypothesis and the resulting generalized t-J model emphasizes that the physics of the conducting state is also determined by a strong coupling physics with superexchange and the consequent RVB physics.

3.2 *Some key experimental facts about Mott transitions*

Standard thought experiment of Mott transition is an adiabatic expansion of a cubic lattice of hydrogen atoms forming a metal. Electron density decreases on expansion and Thomas-Fermi screening length increases; when it becomes large enough to form the first electron–hole bound state, there is a first-order transition to a Mott insulating state, at a critical value of the lattice parameter. This critical value $a_0 \approx 4a_B$, where a_B is the Bohr radius. The charge gap jumps up from zero to a finite Mott–Hubbard gap across the transition (figure 6a), by a feedback process that critically depends on the long-range part of the Coulomb interaction, as emphasized by Mott [43].

Experimentally known Mott transitions are first-order transitions and the insulating side close to the transition point usually have a substantial Mott–Hubbard gap; in oxides this gap is often of the order of an eV. In organics, where the bandwidth are narrow, ≈ 0.25 eV, the Mott–Hubbard gap also has similar value. In view of the finite Mott–Hubbard gap, the magnetism on the Mott insulating side is well described by an effective Heisenberg model with short-range superexchange interactions. There are no low energy charge carrying excitations. That is, we have a strong coupling situation.

What is interesting is that this strong coupling situation continues on the metallic side as shown by optical conductivity studies in Bechgaard [44] and ET salts: one sees a very clear broad peak (a high energy feature) corresponding to the upper Hubbard band both in the insulating and conducting states. The only difference in the conducting state is the appearance of Drude peak, whose strength and shape gives an idea of the number of free carriers that have been liberated (figures 6b and 6c). As the location and width of the Hubbard band has only a small change across the transition, one may conclude that the local quantum chemical parameters such as the hopping matrix elements t's and Hubbard U (corresponding superexchange J) remain roughly the same. This is the basis of our 'strong coupling' hypothesis: a generic Mott insulator metal transition in real system is to a (strong coupling) metallic state that contains superexchange.

As superexchange survives in the conducting state, two neighbouring singly occupied sites of net charge (0,0) cannot decay into freely moving doubly occupied and empty sites (e^-, e^+). Conversely, a pair of freely moving doubly occupied and empty
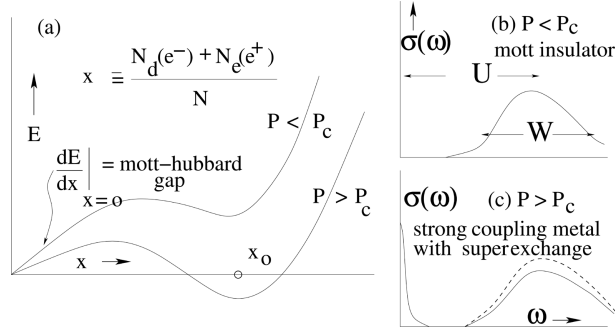
Figure 6. (**a**) Energy of a half-filled band above and below the critical pressure P_c, as a function of $x = \frac{N_d(e^-) + N_e(e^+)}{N}$. Here $N_d(e^-) = N_e(e^+)$ are the number of doubly occupied (e^-) and number of empty sites (e^+); total number of lattice sites N = total number of electrons. Optimal carrier density $x_0 \equiv 2N_0/N$ is determined by long-range part of Coulomb interaction and superexchange energy. (**b**) and (**c**) Schematic picture of the real part of the frequency-dependent conductivity on the insulating and metallic side close to the Mott transition point in a real system. W is the bandwidth.

sites cannot annihilate each other and produce a bond singlet (figure 7). (Recall that in a free Fermi gas, where there is no superexchange, the above processes freely occur.) Superexchange and long-range part of the Coulomb interactions determine the number of self-doped carriers $2N_0$ and their conservation.

3.3 *Two species t-J Model and mean field theory*

The above arguments naturally lead to a generalized t-J model for the conducting side in the vicinity of the Mott transition point

$$H_{\mathrm{tJ}} = -\sum_{ij} t_{ij} P_{\mathrm{d}} c_{i\sigma}^\dagger c_{j\sigma} P_{\mathrm{d}} - \sum_{ij} t_{ij} P_{\mathrm{e}} c_{i\sigma}^\dagger c_{j\sigma} P_{\mathrm{e}} + \text{h.c.}$$
$$- \sum_{ij} J_{ij} \left(\mathbf{S}_i \cdot \mathbf{S}_j - \frac{1}{4} n_i n_j \right), \tag{3.1}$$

operating in a subspace that contains a fixed number N_0 of doubly occupied and N_0 empty sites. The projection operators P_{d} and P_{e} allows for the hopping of a doubly occupied and empty sites respectively in the background $N - 2N_0$ of singly

Figure 7. If superexchange survives on the metallic side, a pair of neighbouring singly occupied sites cannot decay into freely moving doubly occupied and empty sites. The converse is also true.

occupied sites. Here N is the total number of electrons, which is the same as the number of lattice sites. As the Mott–Hubbard gap is the smallest at the Mott transition point, higher-order superexchange processes may also become important and contribute to substantial non-neighbour J_{ij}'s.

Our t-J model adapted to the self-doped Mott insulator has a more transparent form in the slave boson representation $c_{i\sigma}^\dagger \equiv s_{i\sigma}^\dagger d_i + \sigma s_{i\bar\sigma} e_i^\dagger$. Here the chargeons $d_i^\dagger$'s and $e_i^\dagger$'s are hard core bosons that create doubly occupied sites (e^-) and empty sites (e^+) respectively. The fermionic spinon operators $s_{i\sigma}^\dagger$'s create singly occupied sites with a spin projection σ. The local constraint, $d_i^\dagger d_i + e_i^\dagger e_i + \sum_\sigma s_{i\sigma}^\dagger s_\sigma = 1$, keeps us in the right Hilbert space.

In the slave boson representation our t-J model takes a suggestive form:

$$H_{\mathrm{tJ}} = -\sum_{ij} t_{ij}(d_i^\dagger d_j \sum_\sigma s_{i\sigma} s_{j\sigma}^\dagger + e_i e_j^\dagger \sum_\sigma s_{i\sigma}^\dagger s_{j\sigma}) + \mathrm{h.c.}$$
$$-\sum_{ij} J_{ij} b_{ij}^\dagger b_{ij}, \tag{3.2}$$

where $b_{ij}^\dagger = \frac{1}{\sqrt{2}}(s_{i\uparrow}^\dagger s_{j\downarrow}^\dagger - s_{i\downarrow}^\dagger s_{j\uparrow}^\dagger)$ is a spin singlet spinon pair creation operator at the bond ij. It is easily seen that the total number operator for doubly occupied sites $\hat{N}_{\mathrm{d}} \equiv \sum d_i^\dagger d_i$ and empty sites $\hat{N}_{\mathrm{e}} \equiv \sum e_i^\dagger e_i$ commute with the t-J Hamiltonian (eq. (2.2)):

$$[H_{\mathrm{tJ}}, \hat{N}_{\mathrm{d}}] = [H_{\mathrm{tJ}}, \hat{N}_{\mathrm{e}}] = 0. \tag{3.3}$$

That is, $\hat{N}_{\mathrm{d}}$ and $\hat{N}_{\mathrm{e}}$ are individually conserved. In our half-filled band case $N_{\mathrm{d}} = N_{\mathrm{e}} = N_0$. (This special conservation law is true only for our effective t-J Hamiltonian and not for the original Hubbard model.)

This conservation law allows us to make the following statement, which is exact for a particle–hole symmetric Hamiltonian and approximate for the asymmetric case: our generalized t-J model with a fixed number N_0 of doubly occupied sites and equal number N_0 of empty sites has the same many-body spectrum as the regular t-J model that contains either $2N_0$ holes or $2N_0$ electrons. Symbolically it means that $H_{\mathrm{tJ}}(N_0, N_0) \equiv H_{\mathrm{tJ}}(2N_0, 0) \equiv H_{\mathrm{tJ}}(0, 2N_0)$. This means that we can borrow all the known results of t-J model, viz., mean field theory, variational approach, numerical approach etc. and apply them to understand the thermodynamic and superconductivity properties of our self-doped Mott insulator. Response to electric and magnetic field perturbation has to be done separately as the d and e bosons carry different charges, e^- and e^+ respectively.

Another consequence of the above equivalence is shown in figure 8, where we have managed to draw the path of pressure-induced Mott transition in a Hubbard model phase diagram, even though Hubbard model does not contain the crucial long-range interaction physics. The jump from B to C is the first-order phase transition, remembering that in the presence of our new conservation law what decides the spectrum of our generalized t-J model is the total number of e^+ and e^- charge carriers in an equivalent regular t-J model. The horizontal jump is also consistent with our strong coupling hypothesis.
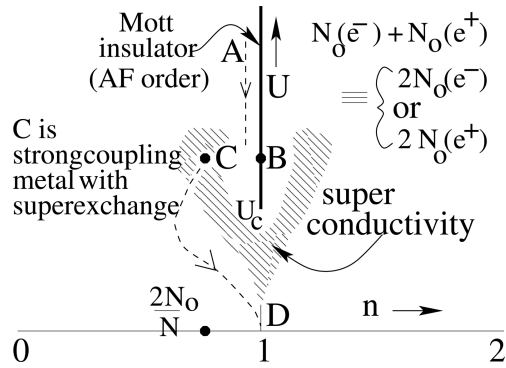
Figure 8. Schematic U–n plane phase diagram for the Hubbard model. ABCD represents the path a real system takes as pressure increases. B to C is the first-order Mott transition, consistent with our strong coupling hypothesis. The point C, from a regular t-J model point of view, is hole-doped at density $n = 2N_0/N$; however, based on our equivalence it corresponds to a half-filled band with a total of $N_0(e^-) + N_0(e^+)$ self-doped carriers.

An important parameter in our modelling is the equilibrium total e^+ and e^- carrier concentration, $x_0 \equiv 2N_0/N$ in our self-doped Mott insulator. This also controls the value of superconducting T_c we will get across the Mott transition point. Estimate of x_0 depends on the long-range part of the Coulomb interaction energy and also the short-range superexchange energy; we will defer this discussion to a later publication. x_0 may also be determined from experiments such as frequency-dependent conductivity by a Drude peak analysis.

Since we have reduced our self-doped Mott insulator problem into a t-J model, superconducting T_c is determined by t, J and x_0, as in the t-J model. If exchange interaction contribution is comparable to the long-range Coulomb contribution, x_0 will be closer to the value that maximizes superconducting T_c. Another important point is the possibility of non-nearest neighbour superexchange J_{ij} processes, which (i) frustrate long-range antiferromagnetic order to encourage spin liquid phase and (ii) increase the superexchange energy contribution to the total energy; this could give a larger superconducting T_c across the Mott transition than expected from a t-J model with nearest-neighbour superexchange. Perhaps an optimal self-doping and sufficiently frustrated superexchange interactions is realized in $(NH_3)K_3C_{60}$ family [38], since Neel temperature $T_n \approx 40$ K and superconducting $T_c \approx 30$ K are comparable.

If the self-doping is small there will be competition from antiferromagnetic metallic phase, stripes and phase separation. For a range of doping one may also get superconductivity from interplane/chain charge disproportionation. If self-doping is very large then the effect of superexchange physics and the consequent local singlet correlations are diluted and the superconducting T_c will become low. This is the reason for the fast decrease of superconducting T_c with pressure in the organics.

3.4 *Predictions and suggestions of new systems*

In what follows we discuss some families of compounds, some old ones and some new ones and predict them to be potential high T_c superconductors, unless some crystallographic transitions or band crossing intervenes and change the valence electron physics drastically. CuO is the mother compound [45] of the cuprate high T_c family. It is monoclinic and CuO_2 ribbons form a three-dimensional network, each oxygen being shared by two ribbons mutually perpendicular to each other. The square planar character from four oxygens surrounding a Cu in a ribbon isolates one nondegenerate valence d-orbital with a lone electron. This makes CuO an orbitally nondegenerate spin-$\frac{1}{2}$ Mott insulator and makes it a potential candidate for our pressure route to high T_c superconductivity. The frustrated superexchange leads to a complex three-dimensional magnetic order with a Neel temperature $\sim$230 K. These frustrations should help in stabilizing short-range singlet correlations, which will help in singlet Cooper pair delocalization on metalization.

As far as electronic structure is concerned, the CuO_2 ribbons give CuO a character of coupled 1d chains. This makes it somewhat similar to quasi-one-dimensional Bechgaard salts, which has a Mott insulator to superconductor transition, via an intermediate metallic antiferromagnetic state as a function of physical or chemical pressure. The intermediate metallic antiferromagnetic state represents a successful competition from nesting instabilities of flat Fermi surfaces arising from the quasi-one-dimensional character. Once the quasi-one-dimensional character is reduced by pressure, nesting of Fermi surface is also reduced and the RVB superconductivity takes over.

If manganite [46] (a perovskite) and fullerites [38] are any guidance, metallization should take place under a pressure of $\sim$tens of GPa's. CuO should undergo a Mott insulator superconductor transition, perhaps with an intermediate antiferromagnetic metallic state. The superconducting T_c will be a finite fraction of the Neel temperature, as is the case with Bechgaard salts or $K_3(NH_3)C_{60}$. Thus, an optimistic estimate of T_c will be 50 to 100 K.

Similar statements can be made of the more familiar La_2CuO_4, insulating YBCO and $CaCuO_2$, the infinite layer compound or the family of Mott insulating cuprates such as Hg- and Tl-based insulating cuprates. Infinite layer compound has the advantage of the absence of apical oxygen and should be less prone to serious structural modifications in the pressure range of interest to us. The quasi-2d-Hubbard model describing the CuO_2 planes does have an appreciable t', making nesting magnetic instabilities weaker. Thus, we expect that on metallization a superconducting state will be stabilized with a small or no antiferromagnetic metallic intermediate state.

The quasi-2d-cuprates have a special advantage in the sense that we may selectively apply ab-plane pressure in thin films by epitaxial mismatch and ab-plane compression. Apart from regular pressure methods, this method [47] should also be tried.

One way of applying chemical pressure in cuprates is to increase the effective electron bandwidth by increasing the band parameters such as t and t' in the Hubbard model. This can be achieved by replacing oxygens in the CuO_2 planes (or in three-dimensional CuO) by either sulphur or selenium, which, because of the

Figure 9. Blue diamond [48] gets its colour from the absorption involving boron acceptor states. As boron doping increases, within the impurity band, singlet bond correlations develop and eventually a dirty RVB superconducting state emerges.

larger size of the bridging 3p or 4p orbitals, increase the bandwidth and at the same time reduce the charge transfer or Mott–Hubbard gap. On partial replacement of oxygen, as $CuO_{2-x}X_x$ in the planes or $CuO_{1-x}X_x$ (X = S, Se) one might achieve metallization without doping.

Some possible new stoichiometric compounds are $La_2CuO_2S_2$, La_2CuS_4 and (infinite layer) $CaCuS_2$ or their Se versions or various solid solutions of the anions. Synthesizing these compounds may not be simple, as the filled and deep bonding state of oxygen 2p orbitals in CuO_2 play a vital role in stabilizing square planar coordination. With S or Se versions these bands will float up and come closer to the Fermi level thereby making square structure less stable. Under pressure or some other nonequilibrium conditions, some metastable versions of these compounds may be produced. One could also optimize superconducting T_c by a judicious combination of pressure-induced self-doping and external doping.

4. Diamond route

Last century witnessed the birth of semiconductor electronics and nanotechnology. The physics behind these revolutionary developments is certain quantum mechanical behaviour of 'impurity state electrons' in crystalline 'band insulators', such as Si, Ge, GaAs, GaN etc. arising from intentionally added (doped) impurities. The present section proposes that certain collective quantum behaviour of these impurity state electrons, arising from Coulomb repulsions could lead to superconductivity, in a parent band insulator, in a way not suspected before. We suggest that superconductivity could be achieved in crystalline insulators such as GaN, ZnO, SiC, NaCl and a host of other insulators, by making use of Coulomb repulsion among the (impurity state) electrons that we introduce intentionally by dopant that are specially chosen. In making the above proposal we are influenced partly (i) by the significant developments in the last 15 years or so in the field of high-temperature
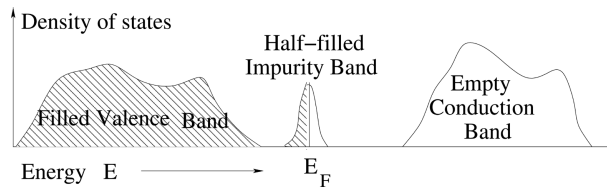
Figure 10. A dopant-induced impurity band. Unlike the broad valence or conduction band the impurity band is a narrow and half-filled strongly correlated system. It can be either on the conducting or insulating side of the Anderson–Mott transition point.

superconductivity in cuprates [1], (ii) a very recent discovery of superconductivity in heavily doped diamond [11–13] and our theory of impurity band superconductivity [6], (iii) and some recent theoretical developments. The logic of our arguments is compelling. The current level of sophistication in solid state technology and combinatorial materials science is very well capable of realizing our proposal and discover new superconductors.

It is indeed interesting that the blueness of blue diamond is due to traces of boron impurities. Visible spectrum, except for blue are absorbed by transitions involving the acceptor states of boron. (Nitrogen impurities make diamond yellow as the impurity levels are much deeper.) As we increase boron doping, blue diamond turns dark. However, according to our theory it starts supporting disordered or dirty RVB states and eventually superconductivity. There should be traces of resonating valence bond states (figure 9) in a blue dimond too!

We suggest that for certain choice of dopants, relatively 'deep level' impurity states can be made to overlap by changing the dopant concentration and cause an impurity band Mott insulator to superconductor transition (figure 10). The spin singlet correlations that are unavoidable in the impurity band Mott insulators are the pre-existing neutral singlets. As we approach transition point, the impurity wave functions overlap more and become 'dense'; consequently the neutral singlets (valence bonds) resonate and a quantum spin liquid phase is formed. Across the Mott insulator to conductor transition, a small density of delocalized holes and electrons are spontaneously generated (required for a self-consistent screening of long-range Coulomb interaction, as suggested by Mott). These carriers delocalize or equivalently a fraction of neutral singlet pairs get charged and delocalize leading to a superconducting state (figure 11).

While the intrinsic randomness in the impurity band systems in general is a great hindrance for metallization from single electron delocalization point of view, electron correlation-based superexchange or pairing of electron into spin singlet states can lead to delocalization of charged singlets resulting in an inhomogeneous superconducting state. Since the number of possibilities is at least as large as the number of available band insulators in nature, the Mott insulating impurity band route we are proposing is worth pursuing!

We also argue that the intrinsic randomness has certain advantages in the sense of reducing the orbital degeneracy of the donor or acceptor impurity states that arise from point group symmetries and valley degeneracy. The degeneracy of the donor or acceptor impurity states are lifted by random strain, electric field and
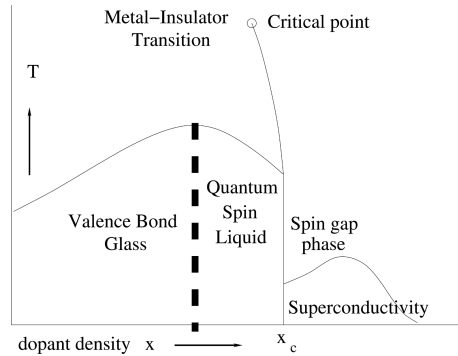
Figure 11. The schematic phase diagram for insulator to metal transition as a function of the dopant density x. For small x we have a valence bond glass, followed by a quantum spin (valence bond) liquid state and a superconducting state. In general, the first-order insulator to metal transition will end in a critical point, whose nature will be strongly influenced by disorder. A spin gap normal state will mark the region near the insulator to metal transition point x_c.

covalency effects. This phenomenon of lifting of orbital degeneracy increases the chance for finding Anderson–Mott insulator to superconductor transition in nature, in comparison to crystalline materials.

Another advantage is the scale of superexchange that nature offers us through our mechanism. It can be as large as the superexchange that exists between copper spins in the cuprates! We will see how this scale of superexchange interaction depends on the band gap and the impurity binding energy of our impurity acceptor or donor states.

The route we are suggesting (diamond route) is likely to be trodden with experimental difficulties (imagine heavily doping a diamond, keeping it still a diamond), hindrances and surprises. One can say with some confidence that it is going to be interesting, fun and rewarding.

4.1 *Impurity state Mott insulators and neutral singlet pairs*

When a dopant atom replaces a host atom in a band insulator, in general localized impurity electronic states are formed. Impurity atom and its interaction with the host determines the nature of the impurity states. In a case like boron doped in diamond, the substituted boron gets nicely accommodated in the sp^3 bonding with the four carbon neighbours; an extra hole of B gets loosely bound to the parent B atom. The impurity eigenfunction is well-described by suitable linear combination of sp^3 band of states. This is at the heart of the well-known effective mass theory of impurity states in semiconductors. The impurity state has a 'hydrogenic envelope' and one defines an effective Bohr radius $a^* \equiv e^2/2\epsilon_0 E_B$, where E_B is the binding energy of the dopant electron–hole and ϵ_0 is the low frequency dielectric constant of the parent insulator.

In all our discussion we use boron impurity in diamond for illustrating our proposal. Our discussion goes through equally well for accepter impurities, such as N or P doped in diamond. Let us assume for simplicity that the ground state of the impurity state is nondegenerate and also ignore effects of low-lying excited impurity states and the conduction band. When we have a finite but dopant density $x = N_d/N$ of dopants (where N_d is the total number dopant atoms that substitute parent atoms of an N-atom lattice); statistically the neutral dopant (D^0) atoms are well-separated with a large mean separation compared to the effective Bohr radius a^*. In this situation we have one dangling electron per D^0 atom, which are practically bound to the respective impurity atoms. This is an impurity state Mott insulator or an Anderson–Mott insulator. What is preventing it from becoming a half-filled impurity band metal is (i) Anderson localization phenomena and (ii) the Mott localization; i.e., energy gain by delocalization of an electron among the impurity states (bandwidth, $\sim W$) is small compared to the energy U (sum of ionization and electron affinity) required to remove an electron from one D^0 atom and put it on another D^0 atom in the impurity state; i.e. to create a real charge fluctuation D^+D^- out of a D^0D^0 pair.

In the Mott insulating state there is virtual charge fluctuation leading to the well-known super/kinetic exchange. That is, virtual transition of a neighbouring neutral dopant atom pair to higher energy (U) polar state

$$D^0(\downarrow)D^0(\uparrow) \to D^-(\uparrow\downarrow)D^+(0) \tag{4.1}$$

leads to an effective Heisenberg coupling between the two dangling spins. In the dilute limit the impurity spin couplings are well-represented by the following Heisenberg Hamiltonian:

$$H_s \approx \sum J_{ij} \left(\mathbf{S}_i \cdot \mathbf{S}_j - \frac{1}{4} \right), \tag{4.2}$$

where $\mathbf{S}_i$ is the spin operator of an electron in the ith impurity atom, $J_{ij} \approx 4t_{ij}^2/U$ is the superexchange between the moments and t_{ij} is the hopping matrix element. As the hopping matrix element t_{ij} falls off exponentially with DD separation $|\mathbf{R}_{ij}|$, the superexchange J_{ij} has a large variation. It should be pointed out that in some special circumstances the superexchange may become ferromagnetic. We focus on situations involving antiferromagnetic coupling. When ferromagnetic coupling dominates, impurity band ferromagnetism may be formed.

4.2 *Valence bond glass to quantum spin liquid cross-over with increased doping*

Dopant atoms form a random lattice with some short-range correlations, leading to a distribution of superexchange coupling among neighbouring spins. A wide distribution of antiferromagnetic exchange constant J_{ij} in a random lattice should normally lead to a spin glass order among impurity spins because of frustration and inability to form a spin arrangement in which every neighbouring pairs of spins are antiparallel. However, as it has been well-established for impurity spins in phosphorus-doped Si, quantum fluctuations, arising from spin-$\frac{1}{2}$ character of the
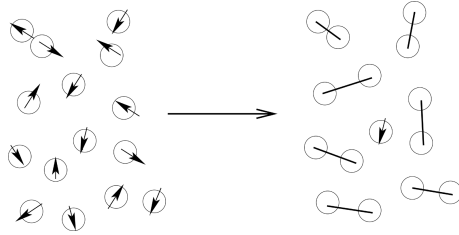
Figure 12. In view of the strong quantum fluctuations the spin-$\frac{1}{2}$ moments form a valence bond glass or frozen spin singlet bond phase rather than a frozen spin glass order.

dangling spins, destabilize spin glass order and leads to the so-called valence bond glass state, depicted schematically in figure 12. This state has neutral singlets dominating the ground state. The random character makes less resonance among the neutral singlets, except in places where there are clustering of the impurity atoms. Further we also get some lone spins, which are weakly coupled to its neighbours. As has been shown both experimentally [49] and theoretically [50], the hierarchical fashion in which spins get singlet coupled as temperature T is reduced, leads to a non-Curie form for the spin susceptibility $\chi_{\text{spin}} \sim \frac{1}{T^{1-\alpha}}$, where $\alpha > 0$.

In our resonating valence bond (RVB) mechanism of Mott insulator to superconductor transition, the following are the minimal requirements for superconductivity: (i) a spin-half Mott insulating reference state and (ii) antiferromagnetic superexchange leading to spin singlet correlations and valence bond resonance. The resonating singlets are the pre-existing Cooper (neutral) pairs. Absence or minimal orbital degeneracy is important lest (a) Hunds rule intervenes and stabilizes metallic magnetic states or (b) Jahn–Teller effect intervenes and trap doped carriers or stabilize charge/orbital orders. While lower dimensionality is helpful, it is not absolutely important in RVB theory.

As we approach the metal–insulator transition, with increase in dopant concentration, at least three phenomena take place simultaneously: (i) the impurity state wave functions overlap more and electrons try to overcome Anderson localization to form extended one-particle states and (ii) the mean value of neighbouring superexchange constant J grows and its distribution becomes narrower and (iii) because of the reduction of the mean charge gap, multispin exchange processes start contributing. We hypothesize that the net effect is a valence bond delocalization and formation of a percolating region of quantum spin liquid (figure 13). The above two processes are connected. A quantitative analysis of them is involved and is out of the scope of the present paper. However, it should be pointed out that the above becomes very plausible, once we recognize that the impurity wave functions are dense and overlapping (figure 13) in the sense that at the Mott transition point the mean inter-impurity distance and the effective Bohr radius become comparable – their spatial pattern is like a frozen configuration of a dense fluid of hardspheres, rather than a dilute gas.

In view of the above, there is enhanced valence bond resonance and a valence bond glass crosses over continuously to a valence bond liquid in the region just prior to the Mott transition point. In other words our hypothesis states that for
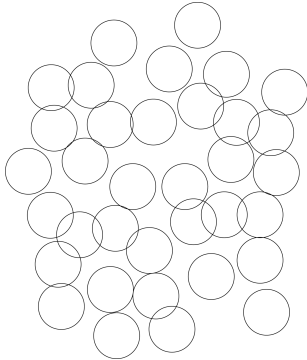
Figure 13. The impurity wave functions overlap become dense and the distribution of nearest neighbour super-exchange becomes narrower, leading to a quantum spin liquid or valence bond liquid.

low energy scales, we may view the many-body insulating spin state just close to the Mott transition point as a nonrandom homogeneous quantum spin liquid state, in a first approximation. If the dopants were to form a regular three-dimensional lattice, the spin liquid state will be unstable towards long-range antiferromagnetic order.

In the above sense we have a system, which has resonating neutral singlets, or preformed Cooper pairs, that is ripe for superconductivity. We can introduce delocalized charges into the systems and get superconductivity in two ways: (i) by external doping, through partial compensation and (ii) self-doping, by increasing the dopant concentration beyond the insulator to metal critical point. The intrinsic randomness will introduce an inhomogeneous superconducting state.

4.3 *Mott insulating quantum spin liquid to a superconductor transition*

Once we have made a hypothesis of homogeneous quantum spin liquid state, the issue of Mott insulator in a quantum spin liquid to a metal transition becomes similar to the analysis made by the present author in the context of Mott insulator to superconductor transition in crystalline organics and other systems [5]. We will also argue that an intrinsic randomness in our case is not a serious hindrance for Mott insulator–superconductor transition; on the contrary it has certain advantages!

Our theory of Mott insulator to superconductor transition closely followed Mott's argument for insulator to metal transition but with two important and new ingredients: (i) unlike Mott, who focussed on charge delocalization, we also consider spin physics and singlet correlations on the conducting side and (ii) unlike Brinkman and Rice and other authors, we view the conducting side as a Mott insulator with a small density of 'self-doped' carriers, rather than a half-filled band of a Fermi liquid with a very large effective mass. That is, a small but equal density of 'self-doped' carriers, doublons (D^-) and holons (D^+) delocalize in the background of the resonating singlets (figure 14). In the conducting state superexchange survives because the upper and lower Hubbard band features persist even after metallization, as suggested by frequency-dependent conductivity experiments in the organics [5], for example. Survival of upper and lower Hubbard band means presence of local moments in the metallic state with superexchange interactions. Schematically, the

neutral dopant of the impurity state Mott insulator $N_{\rm d}$ gets separated, across the Mott insulator to metal transition as follows:

$$
\begin{aligned}
N_{\rm d} &\rightarrow (1-x)N_{\rm d} &+& \quad \frac{x}{2}N_{\rm d} &+& \quad \frac{x}{2}N_{\rm d} \\
[D^0] &\rightarrow (1-x)[D^0] & & \quad \frac{x}{2}[D^-] & & \quad \frac{x}{2}[D^+]
\end{aligned}
$$

Creation of a self-doped Mott insulating state (that is, a metallic state with surviving superexchange) crucially depends on the first-order character of the Mott transition, which in turn depends on the long-range nature of the Coulomb interaction. That is, a finite global charge gap that exists on the insulating side survives as a local charge gap on the metallic side, in the presence of a small density of self-doped carriers. The value of the charge gap at the insulating side at the insulator to metal transition point determines the magnitude of the superexchange on the metallic side. Further, self-consistency demands that larger the charge gap at the transition point lesser is the self-dopant charge density. A Hubbard model, which generically produces a continuously vanishing charge gap at the insulator to metal transition point, is thus not capable of describing a self-doped Mott insulating state.

The dynamics of spin and charges in the above situation is summarized by the following effective Hamiltonian, which we called as a 2-species t-J model (eq. (3.1)); adapted to our present situation the Hamiltonian is:

$$
\begin{aligned}
H_{\rm 2tJ} = &- \sum_{ij} t_{ij} P_{\rm d} c_{i\sigma}^\dagger c_{j\sigma} P_{\rm d} - \sum_{ij} t_{ij} P_{\rm e} c_{i\sigma}^\dagger c_{j\sigma} P_{\rm e} + {\rm h.c.} \\
&- \sum_{ij} J_{ij} \left(\mathbf{S}_i \cdot \mathbf{S}_j - \frac{1}{4} n_i n_j \right) + \sum_i \epsilon_i c_\sigma^\dagger c_\sigma.
\end{aligned}
\tag{4.3}
$$

Here ϵ_i's represent site energies of the localized impurity states. The presence of a special form of kinetic energy and superexchange term tells us that the system is a Mott insulator that is self-doped. The conventional kinetic energy gets modified and we get doublon and holon hopping terms. A part of the kinetic energy term that represents annihilation of a doublon and a holon into two spinons (figure 7) does not appear in the above effective Hamiltonian, as its effect has been already taken into account in generating the superexchange terms.

After years of effort both from theoretical side and experimental side, there is a good consensus [51,52] for the validity of one band t-J model as a reasonable model describing the low energy physics such as superconductivity and magnetism. In spite of a variety of theoretical efforts, no rigorous proof exists for superconductivity in the t-J model. As t-J model is proved to be the right model from experiment point of view, in a sense experiments provide strong support for the existence of superconductivity in a 2d t-J model. However, it is fair to say that the RVB mean field theory has been very successful in describing qualitatively the overall phase diagram and even the symmetry of the order parameter. Years of efforts on variational wave functions have also given a very good support for the RVB mean field scenario and existence of superconductivity. Our current proposal of impurity band Mott insulator route to high $T_{\rm c}$ superconductivity brings in an additional feature namely randomness. Here we can also invoke some kind of Anderson's theorem
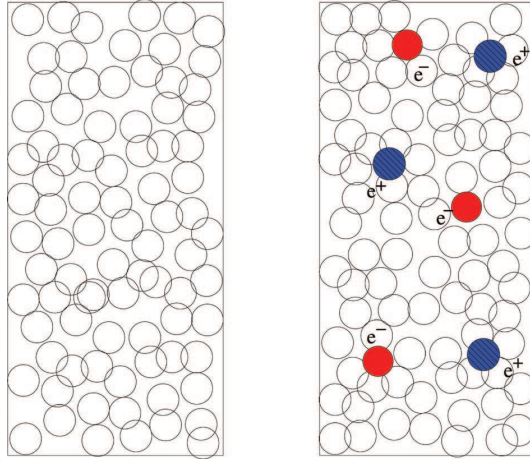
Figure 14. The nominal charge states of the dopant atoms on the insulating and metallic side in the vicinity of the insulator to metal transition point. On the insulating side we have no real charge fluctuations; superexchange leads to a neutral spin liquid. On the metallic side, long-range interaction manages to self-dope a small and equal density of negative (red, doublon) and positive (blue, holon), even while maintaining the local Mott insulating and spin singlet character everywhere.

and suggest that randomness gets renormalized to small values when we consider pairing among time-reversed states rather than Bloch states. The STM (scanning tunnelling microscopy) analysis in superconducting boron-doped diamond [53] do show strong spatial inhomogeneity in the order parameter, and at the same time the system exhibits a robust bulk superconductivity. It has been suggested that the (singlet) valence bond maximization [26] holds the key to superconductivity, and it is unlikely that the randomness will completely eliminate superconductivity.

4.4 *Estimation of impurity bandwidth W, critical doping x_c and superexchange J*

Effective mass theories have been successful in determining the insulator to metal transition point for various shallow dopants [54]. For deep level impurities the problem is hard. However, one can use various quantum chemical insights and quantum chemical calculations and estimates. With the availability of powerful computers it is possible to infer the bandwidth and superexchange J among impurity states, for the specific system under consideration, using LDA method and supercell analysis. The values will be system-specific and we can choose systems that give satisfactory W and J. What is satisfactory will be discussed in what follows. As emphasized [55], the difference in spatial extent of the impurity state wave function in D^- and D^+ will modify the superexchnge constant and also introduce asymmetry between doublon and holon hopping matrix elements.

   Using available data on the impurity states of substitutional nitrogen impurity in diamond we estimate that close to the critical point the deep level nitrogen impurity states offers a substantial antiferromagnetic superexchange ∼0.5 eV.

4.5 *Estimation of superconducting T_c*

In RVB mechanism, superconductivity is a robust phenomenon and estimation of T_c should be relatively easy, provided our analysis captures the robust character correctly. Historically two approaches are available for estimating T_c: (i) Bose condensation of a fraction x of the charged singlet bonds in an RVB state (x is the self- or external doping fraction) and (ii) estimating T_c directly by various approximate analysis of the large U Hubbard model. The Bose condensation approach gives the famous dome phase diagram for T_c in the x–T plane. That is, superconductivity is basically a Bose–Einstein condensation phenomenon of a dilute liquid of charged valence bonds. The charged valence bonds have a short-range repulsion. Consequently for 2d we have a Kosterlitz–Thouless transition with a T_c given by

$$k_B T_c \approx \frac{2\pi \hbar^2 n_d}{m_d^*}. \tag{4.4}$$

In 3d the expression for the Bose–Einstein condensation temperature of noninteracting Bose gas gives an estimate of T_c:

$$k_B T_c \approx \frac{2\pi}{(2.612)^{2/3}} \frac{\hbar^2 n_d^{2/3}}{m_d^*}. \tag{4.5}$$

Here m_d^* and n_d are the effective mass and density of the self-doped or externally doped carriers. For a given x, the background singlet pairing among spins continue till the so-called spin gap temperature T^* scale. That is, the above formulae are good at small dopings, when T_c is small compared to the temperature scale above which RVB singlets are unstable. Earlier RVB mean field theory and later developments provide an estimate of T^* as follows:

$$k_B T^* \sim J_{\text{eff}} e^{-\frac{1}{\rho_0 J_{\text{eff}}}} \sim J(1 - \alpha x), \tag{4.6}$$

where the density of states at the Fermi energy of the spinon Fermi surface $\rho_0 \approx 1/J_{\text{eff}}$ and the effective interaction among spinons is $J_{\text{eff}} \approx J(1 - \alpha x)$, where $\alpha \approx W/J$. The spin gap temperature provides a natural cut-off for Bose condensation of charged singlet bonds. As a result, we have the dome-like behaviour [56] of the superconducting T_c in the x–T plane, with maximum T_c at an optimal doping.

In the second approach one directly analyses the large U Hubbard model for superconductivity, using various approximate methods. We will not go into the details of the result. However, what one finds is that the superconducting T_c at optimal doping is in the range $W/100$ to $W/50$. For example, for cuprates the bandwidth $W \approx 1$ eV, leading to a T_c in the range 100 K. The value of T_c in the above also relatively insensitive to the value of U, provided $U > W$, the bandwidth.

From the above discussions we conclude that the impurity bandwidth W provides an important scale for superconducting T_c, in the insulator metal transition region, provided the Mott insulating character survives (that is $U > W$) in the metallic state in the presence of a small density x of self-doping. When the self-doping or external doping reaches the optimal value ($x \approx 0.15$ for cuprates) we will get maximum superconducting T_c.

Keeping in mind the randomness in our impurity band Mott insulators, we will get a rough estimate of T_c for boron-doped diamond. For the impurity band to retain its identity the bandwidth should be less than the binding energy $\epsilon_0 \approx 0.36$ eV. Taking into account the tail in the density of states arising from randomness we can take an effective bandwidth, $W \approx 0.18$ eV, which is about half the above value. This gives us a maximum possible value of T_c in the range 10 to 30 K.

This is indeed interesting. In boron-doped diamond, experimentally we still do not have a good control over homogeneous substitutional doping. There is also difficulty in determining density of boron substitution, as a fraction of boron's go into interstitial sites. It is likely that we have not reached the maximum possible T_c in boron-doped diamond. Further increase in T_c may be possible, according to our estimates.

When we apply the above estimation method for phosphorus-doped Si we get a superconducting T_c, which is at least a factor of 5 lower compared to boron-doped diamond. It follows from the fact that phosphorus is a shallow donor with a binding energy of about 50 meV. Correspondingly the impurity bandwidth in the vicinity of the insulator to metal transition point is considerably low compared to boron impurity band in diamond. Recent experiments in heavily boron-doped Si and SiC have yielded low T_c superconductivity [57,58]. The low value of T_c is consistent with the small impurity state binding energy. Further, in these experiments one is far away from the insulator to metal transition point, as the doping level is high. So it is likely that the impurity bands have disappeared. In such a situation the doped Mott insulator picture that we are advocating is clearly not applicable and an electron–phonon mechanism might suffice. On the other hand, if one does find superconductivity at the metal insulator transition point (like in boron-doped diamond), the strong correlation mechanism we are suggesting is inescapable in that neighbourhood.

4.6 *Advantages of disorder for superconductivity*

While randomness inherent in our impurity band approach can decrease super-conducting correlations, it has the following advantage. It is known from the two decades of experimental and theoretical works in cuprates that in doped Mott insulators there are competing orders such as valence bond localization, spin or charge order or chiral orders. Any encouragement of these competing orders from the lattice such as a strong electron–lattice coupling and valence bond localization will decrease superconducting T_c resulting from a reduced valence bond resonance. In general a random lattice frustrates real space spin or charge orders. It also frustrates d-wave superconducting order for example. However, they do not frustrate the extended-S superconducting order, one of the stable solution of RVB mean field theory [23].

4.7 *Ways to increase T_c*

In the last section we have seen that the maximum value of superconducting T_c in our strong correlation-based impurity band mechanism is primarily measured by the impurity bandwidth. The maximum allowed impurity bandwidth, in turn, is

limited by the impurity state binding energy. So any search for higher T_c should also focus on impurity binding energy large compared to the case of boron-doped diamond, the best available impurity band superconductor, as explained by our theory.

First we will discuss optimization of T_c in the case of diamond. Heavy doping of any foreign atom into diamond is notoriously hard. Boron continues to be the dopant with the highest doping density. Doping with nitrogen is a very interesting possibility, however filled with formidable experimental difficulties. We have estimated parameters such as critical nitrogen concentration for insulator to metal transition and maximum possible transition temperature for nitrogen-doped diamond. Experimentally it is known that substitutional nitrogen is a donor with a high binding energy of about 1.5 eV, about four times larger than that of boron in diamond. Correspondingly we estimate a large T_c of about 50 to 120 K.

However, there are quantum chemical constraints and lattice instabilities which prevent attaining the required heavy doping regime for nitrogen. The critical doping concentration $x_c > 0.2$ necessarily for insulator to metal transition is too large to be experimentally achieved at the present moment. That is, a stable solid solution $C_{1-x}N_x$ that also maintains a diamond lattice structure does not seem to exist for the range of x of interest to us. The nitrogen dopants form pairs, or generate nitrogen-vacancy pairs or create a large Jahn–Teller distortion etc.

In addition to the stabilization of the valence bonds through electron correlation that we have suggested, it has been suggested that the high frequency C–C bond vibration in boron-doped diamond will help in stabilizing and delocalizing the valence bonds [59] and hence increasing T_c.

Other authors have argued that electron–phonon interaction is the major contributor to pairing and superconductivity. As an evidence, observation of isotope effect [60] is presented. It is important to note that isotope effects of similar magnitude could appear through modification of the hopping matrix element of the impurity band by change in zero point oscillations. This is known in the case of cuprates [61]. We find that similar arguments can be offered for the observed isotope effect [62].

Nature offers us a wealth of band insulators with large band gaps. It will be very interesting to explore the possibility of creating impurity band Mott insulators with a larger bandwidth. There has been one theoretical suggestion by Alaeia *et al* [63], that a high density of vacancies in diamond can form an impurity band and that our superconductivity mechanism might work. On the experimental side, inspired by our mechanism, there has been a collective effort 'super hydrogenic state' project headed by Venkatesan [64] to create impurity band Mott insulator and search for superconductivity.

The choice of dopants is also very important. So far, inspired by boron-doped diamond we have been talking about p-block dopants such as boron and nitrogen. The traditional transition metal or rare earth metal can easily form deep level impurity states. However, because of electron–electron interaction effects in the partially filled impurity d or f shell, Hund coupling stabilized high spin states and ferromagnetic, magnetic or spin glass states will be the ground state. The multiple charge states associated with transition metal deep impurity states also brings in features, which are hard to comprehend at the present moment from

superconductivity point of view. Transition metals on the border of the row such as Sc, Ti and Cu are good candidates for dopants. Monovalent alkali metals and noble metals such as Au, Ag are also good candidates. While it may be difficult to accommodate the above dopants in diamond for quantum chemical reasons, various oxides and other insulators might offer opportunities for heavy doping and creation of impurity band Mott insulators. So one should try a variety of large band gap band insulators.

5. Graphene route

So far we have been focussing on Mott insulators and doped Mott insulators, which are strongly correlated systems. Will superconductivity survive in systems that have intermediate correlations? Theoretical analysis of repulsive Hubbard model in two dimensions on a square lattice shows that superconductivity survives even for intermediate U, with a value of T_c that is not significantly reduced compared to the strong coupling situation. What seems to be important is the addition of short-range spin singlet correlations. Singlet stabilization continues even at intermediate values of U. Further, superconducting T_c in RVB theory depends on bandwidth, through the delocalized dopant mass. Thus higher the bandwidth, higher is the superconducting T_c. This gives us hope for having high T_c superconductivity in systems with high bandwidth and intermediate electron correlation. We have found, based on our theory, that the currently popular graphene satisfies the above criteria and has the potential to become room temperature superconductor. Our work, which will be presented below, encourages a search for new broadband low-dimensional systems for high T_c superconductivity. We call this graphene route.

Superconductivity at room temperature is at present a dream. Attempts to make it real has led to the discovery of 'high T_c' superconductivity in layered materials like cuprates [1,3], organic superconductors, MgB$_2$ [65] and most recently, Fe pnictides [14,15] family. Graphene, a semi-metal, is a single-atom thick layer of carbon net [66–68]. A newly discovered method to cleave and isolate single or finite number of atomic layers of graphene, its mechanical robustness and novel electrical properties has caught the attention of the scientific and nanotechnology community. Undoped graphene is a semi-metal and does not superconduct at low temperatures. However, on 'doping optimally' if graphene supports high T_c superconductivity it will make graphene even more valuable from basic science and technology points of view.

Here we build on a seven-year-old suggestion of Baskaran [69] (GB) of an electron correlation-based mechanism of high T_c superconductivity for graphite-like systems. GB combined, through a new model Hamiltonian, conventional band theory for graphene and Pauling's old RVB theory which emphasized pair-wise electron correlation. The model predicted vanishing T_c for undoped graphene, consistent with experiments, in view of vanishing density of states at the Fermi level. It predicted high T_c superconductivity for doped graphene, when density of states reaches some optimal value. Very recently, Black-Schaffer and Doniach [70] studied GB's effective Hamiltonian systematically using mean field theory, for graphitic systems. They obtained results for superconducting T_c for a range of doping and further found an unconventional $d+id$ order parameter symmetry as low energy mean field

solution. Recent renormalization group analysis of Honerkamp confirms the mean field $d + id$ instability, away from half filling. Other authors have studied the possibility of superconductivity based on electron–electron and electron–phonon interactions [68,71–74].

Since there is an encouraging signal for high T_c superconductivity in the phenomenological GB model, it is important to establish this possibility by studying a more basic and realistic model. So we analyse the repulsive Hubbard model that describes the low energy properties of graphene. We construct variational wave functions motivated by RVB physics, and perform extensive Monte Carlo study incorporating crucial correlation effects. This approach which has proved to be especially successful in understanding the ground state of cuprates, clearly points to a superconducting ground state in doped graphene. Our estimate of the Kosterlitz–Thouless superconducting T_c is of the order of room temperature.

5.1 *Model for superconductivity in graphene*

Low energy electrical and magnetic properties of graphene are usually described by a tight binding model of free electrons on a honeycomb lattice with a single $2p_z$ orbital per carbon atom:

$$\mathcal{H}_0 = -\sum_{\langle ij \rangle} t_{ij} c^\dagger_{i\sigma} c_{j\sigma} + \text{h.c.} \tag{5.1}$$

Here, i labels atomic sites, $c_{i\sigma}$ is an annihilation operator for an electron with spin σ at site i, $n_{i\sigma}$ is the number operator at site i of σ spin electrons, $t \approx 2.5$ eV is the hopping matrix element. The unique band structure of the above model leads to a 'Dirac cone'-type of spectrum for electron motion close to K and K' points in the Brillouin zone and linearly vanishing density of states at the Fermi level, for undoped graphene.

Pauling, on the other hand, emphasized covalent $p\pi$ bond (pair correlation) between two electrons on neighbouring carbon atoms and suggested a resonating valence bond (RVB) theory for graphene. In the modern parlance, we will say that Pauling emphasized electron correlation, because he completely ignored charge fluctuations. In fact, Pauling's RVB state describes a Mott insulator, as opposed to a weakly correlated electron state, where charge fluctuations occur freely. Pauling's approach has been extremely useful to understand low energy physics of $p\pi$ bonded planar molecular system, where configurations corresponding to charge fluctuations are suppressed by Coulomb repulsions. For example, the large energy difference of $\sim$3 eV between the first spin triplet and spin singlet excitations (exciton) in benzene can be easily explained by the strong correlation phenomena related to Mott physics. Such a spin triplet and singlet exciton energy splitting is a hallmark of finite size $p\pi$ bonded systems. Indeed, it is customary in quantum chemistry literature to use a spin-$\frac{1}{2}$ Heisenberg model with an effective nearest-neighbour exchange J (≈ 2.5 eV) and smaller non-neighbour couplings to describe the low energy excited states of $p\pi$ bonded planar molecular systems.

One had a feeling that as we go from benzene to graphene (zero to two dimensions) Coulomb repulsion will get renormalized to zero and we will be left with

essentially a free electron situation. However, it was shown by Akbar and GB [76] that on-site Coulomb repulsion (Hubbard U) for graphene will lead to a gapless spin-1 collective mode branch that survives for arbitrarily small repulsive U. It is a nonperturbative effect indicating the survival of a nonzero effective nearest-neighbour J in graphene.

In order to study graphite-like systems for superconductivity, GB introduced a phenomenological model, where the band theory description was supplemented with a nearest-neighbour singlet pairing term, in order to incorporate Pauling's RVB correlation:

$$\mathcal{H}_{\mathrm{GB}} = -\sum_{\langle ij \rangle} t_{ij} c_{i\sigma}^\dagger c_{j\sigma} + \text{h.c.} - J \sum_{\langle ij \rangle} b_{ij}^\dagger b_{ij}, \qquad (5.2)$$

where $b_{ij}^\dagger = \frac{1}{\sqrt{2}}(c_{i\uparrow}^\dagger c_{j\downarrow}^\dagger - c_{i\downarrow}^\dagger c_{j\uparrow}^\dagger)$ creates a spin singlet on the $\langle ij \rangle$ bond. J (> 0) is a measure of singlet or valence bond correlations emphasized by Pauling, i.e., a nearest-neighbour attraction in the spin singlet channel. In the present paper we call it a 'bond singlet pairing' (BSP) pseudopotential. The parameter J was chosen as the singlet triplet splitting in a 2-site Hubbard model with the same t and U, $J = \frac{1}{2}[(U^2 + 16t^2)^{1/2} - U]$. As U becomes larger than the bandwidth, this psuedopotential will become the famous superexchange characteristic of a Mott insulator.

This model [69] predicts that undoped graphene is a 'normal' metal. The linearly vanishing density of states at the chemical potential engenders a critical strength J_{c} for the BSP to obtain a finite mean field superconducting T_{c}. The parameter J for graphene was less than the critical value, and undoped graphene is not a superconductor despite Pauling's singlet correlations. Doped graphene has a finite density of state at the chemical potential and a superconducting ground state is possible. Black-Schaffer and Doniach [70] confirmed GB's findings in a detailed and systematic mean field theory and discovered an important result for the order parameter symmetry. They found that the lowest energy mean field solution corresponds to $d + id$ symmetry, an unconventional order parameter, rather than the extended-s solution. The value of mean field T_{c} obtained was above room temperature scales.

As results of the mean field theory of GB Hamiltonian are spectacular we wish to go to the more basic repulsive Hubbard model and confirm this important prediction. We start with the Hubbard model

$$\mathcal{H}_{\mathrm{H}} = -\sum_{\langle ij \rangle} t_{ij} c_{i\sigma}^\dagger c_{j\sigma} + \text{h.c.} + U \sum_i n_{i\uparrow} n_{i\downarrow} \qquad (5.3)$$

with $U \approx 6$ eV for graphene [75]. We construct a many-body variational ground state and optimize it using variational quantum Monte Carlo (VMC) [77]. The ground state is a suitably modified mean field solution of the GB model to take care of repulsive U, containing BCS factors $u(\boldsymbol{k})$ and $v(\boldsymbol{k})$, which are functions of the single particle band dispersion $\varepsilon(\boldsymbol{k}) - \mu_f$ and the gap function $\Delta(\boldsymbol{k}) = \sum_{\alpha=1,2,3} \Delta_\alpha \mathrm{e}^{ik} \cdot a_\alpha$. Here a_α are the three nearest-neighbour lattice vectors of any site. The pair function is chosen to be $\Delta_\alpha = \Delta \mathrm{e}^{i2\pi(\alpha-1)/3}$, to reflect the $d + id$ symmetry.
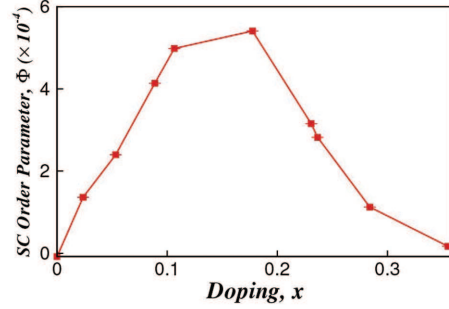
Figure 15. Doping dependence of superconducting order parameter Φ as obtained from VMC calculation of the Hubbard model on a honeycomb lattice for $U/t = 2.4$.

5.2 *Variational Monte Carlo studies*

We start with the N-particle projected BCS state $|\mathrm{BCS}\rangle_N$ with an appropriate number N of electrons. If we work with a lattice with L sites, this corresponds to a hole doping of $1 - N/L$. Our candidate variational ground state $|\Psi\rangle$ is now a state with a partial Gutzwiller–Jastrow projected [78,79] state, containing the variational Gutzwiller factor g, the Hartree shift μ_f and the gap parameter Δ:

$$|\Psi\rangle = g^{\mathcal{D}}|\mathrm{BCS}\rangle_N. \tag{5.4}$$

Here $\mathcal{D} = \sum_i (n_{1\uparrow}^a n_{1\downarrow}^a + n_{1\uparrow}^b n_{1\downarrow}^b)$ is the operator that counts the number of doubly occupied sites. The ground state energy $\langle\Psi|\mathcal{H}_{\mathrm{H}}|\Psi\rangle$ is calculated using quantum Monte Carlo method [77], and is optimized with respect to the variational parameters.

We monitor superconductivity by calculating the following correlation function using the optimized wave functions

$$F_{\alpha\beta}(\mathbf{R}_i - \mathbf{R}_j) = \langle b_{i\alpha}^\dagger b_{j\beta}\rangle, \tag{5.5}$$

where we define $b_{i\alpha}^\dagger$ as the bond singlet operator of a site connected to the nearest-neighbour in the α direction. The superconducting order parameter, the off-diagonal long-range order (ODLRO), is

$$\Phi = \lim_{|\mathbf{R}_i - \mathbf{R}_j| \longrightarrow \infty} F(\mathbf{R}_i - \mathbf{R}_j), \tag{5.6}$$

where $F(\mathbf{R}_i - \mathbf{R}_j) = \sum_\alpha F_{\alpha\alpha}(\mathbf{R}_i - \mathbf{R}_j)$. All results we show in this paper are performed on lattices with 13^2 unit cells.

The superconducting order parameter Φ as a function of doping, calculated for physical parameters corresponding to graphene, obtained using the optimized wave function is shown in figure 15. Remarkably, a 'superconducting dome', reminiscent of cuprates [80], is obtained and is consistent with the RVB physics. The result indicates that undoped graphene had no long-range superconducting order consistent with physical arguments and mean field theory [70] of the phenomenological GB
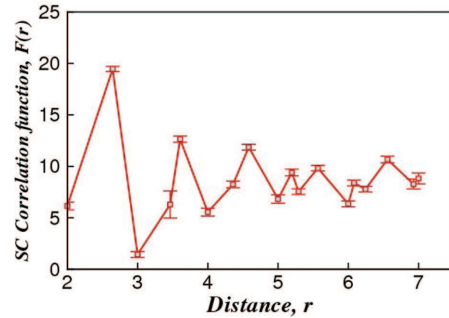
Figure 16. Cooper pair correlation functions and extraction of coherence length.

Hamiltonian. Interestingly, the present calculation suggests an 'optimal doping' x of about 0.2 at which the ODLRO attains a maximum. These calculations strongly suggest a superconducting ground state in doped graphene.

We now further investigate the system near optimal doping in order to estimate T_c. Figure 16 shows a plot of the order parameter function $F(r)$ as a function of the separation r. The function has oscillations up to about six to seven lattice spacings and then attains a nearly constant value. From an exponential fit (figure 16) one can infer that the coherence length ξ of the superconductor is about six to seven lattice spacings. A crude estimate of an upper bound of transition temperature can then be obtained by using results from weak coupling BCS theory, using $k_b T_c = \hbar v_F / (1.764 \pi \xi)$. Conservative estimates give us $k_b T_c = t/50$, i.e., T_c is about twice room temperature. Evidently, this is an upper bound, and an order of magnitude lower than the mean field theory estimates of Black-Schaffer and Doniach [70]. Further improvement of our estimate of T_c becomes technically difficult.

It is interesting to use results of Hubbard model on a square lattice that captures cuprate physics and get some idea about hexagonal lattice graphene. In the case of cuprates at optimal doping, a similar estimate of the coherence length ξ is about two to three lattice spacings [80]. However, the hopping scale is nearly a magnitude lower giving an estimate of $T_c \sim 2 T_{\text{Room}}$ for graphene. Again, this provides further support for the possibility of high temperature superconductivity in graphene.

RVB theory is about superconductivity in Hubbard model in the strong coupling limit, namely the case of doped Mott insulators. Neutral graphene is a semi-metal and not a Mott insulator; what is remarkable is that doping a semi-metal leads to superconductivity. This means that at least in two dimensions, the physics of strong coupling regime survives in the intermediate [81,82] and weak coupling [83] regime. Indeed this is known in the case of square lattice repulsive Hubbard model in the weak coupling limit: various approaches, including functional RG leads to a d-wave superconducting instability away from half filling.

Let us go into the physical origin of our superconductivity in the weak or intermediate coupling regime close to half filling, using the notion of correlation hole. In a tight binding model, correlation hole development corresponds to avoidance of double occupancy at a given Wannier orbital. The Gutzwiller factor $1 - g$ is a measure of correlation hole in the ground state and Δ a measure of nearest-neighbour singlet

correlations. When $U = 0$, there is no correlation hole and no singlet correlations. Our result simply indicates that correlation hole development is accompanied by increased nearest-neighbour singlet correlations Δ. This is straightforward in the strong coupling limit, where one has a complete correlation hole at low energy scales and a corresponding superexchange. Our results indicate that this survives in the weak coupling limit as well. Since our problem is lower (two)-dimensional Hubbard U is not renormalized to zero. Instead, repeated scattering in the spin singlet channel, through Hubbard U, entangles spins pair-wise into singlet states. Or it generates an effective superexchange J, even in the weak coupling regime.

Our prediction of high T_c superconductivity raises some obvious questions. Intercalated graphite can be viewed as a set of doped graphene layers that have a strong three-dimensional electronic coupling. Maximum T_c obtained in these systems is around 16 K [84,85]. Systems such as CaC_6 has a doping close to optimal doping that we have calculated. Why is T_c so low? On the other hand, superconducting signals with a T_c around 60 K and higher have been reported in the past in pyrolitic graphite containing sulphur [86,87]. A closer inspection reveals that for systems like CaC_6 (i) an enhanced three-dimensionality arising through the intercalant orbitals makes the effect of Hubbard U less important (effect of U for a given bandwidth progressively becomes important as we go down in dimensions) and (ii) encouragement of charge density wave order arising from the intercalant order. Sulphur-doped graphite, however, gives a hope that there is a possibility of high temperature superconductivity. Our present theoretical prediction should encourage experimentalists to study graphite from superconductivity point of view systematically, along the line pioneered by Kopelevich and collaborators [87]. In the past there have been claims (unfortunately not reproducible) of Josephson-like signals in graphite- and carbon-based materials [88]. Again, our result should encourage the revival of studies along these lines.

Simple doping of a freely hanging graphene layer by gate control to the desired optimal doping of 10–20% is not experimentally feasible at the present moment. It will be interesting to discover experimental methods that will allow us to attain these higher doping values. A simple estimate shows that a large cohesion energy arising from the strong σ bond that stabilizes the honeycomb structure will maintain the structural integrity of graphene. At low doping, one could uncover the hidden superconductivity by disorder control and study the Cooper pair fluctuation effects.

The discovery of time reversal symmetry breaking $d + id$ order [70] for the superconducting state, within our RVB mechanism is very interesting. This unconventional order parameter has its own signatures in several physical properties: (i) spontaneous currents in domain walls, (ii) chiral domain wall states, (iii) unusual vortex structure and (iv) large magnetic fields arising from the $d = 2$ angular momentum of the Cooper pairs, which could be detected by μSR measurements. Suggestions for experimental determination of such an order by means of Andreev conductance spectra have been made by Jiang [89].

6. Double RVB route

In all the previous discussions we focussed on strongly correlated systems that have odd number of valence electrons per atom, most of them spin-$\frac{1}{2}$ Mott insulators.

Recently, there was a surprise. LaOFeAs, a strongly correlated even electron system (Fe^{2+} in $3d^6$ configuration) exhibited high T_c superconductivity [15,90–92] on doping. What is striking is that the overall phase diagram and several properties closely resemble superconducting cuprates. We have recently suggested [8] evidence for the system to be on the verge of becoming a spin-1 Mott insulator and developed a theory. Either internal pressure or external doping add carriers to the spin-1 Mott insulator. Further analysis reveals that this system may be viewed as two interacting spin-$\frac{1}{2}$ Mott insulators. As we go to higher spin Mott insulators such as $LaMnO_3$ doping leads to ferromagnetism through double exchange mechanism. We show that spin-1 Mott insulators could escape double exchange ferromagnetism under a broad condition and lead to a superconducting state. This has led to our notion of double RVB state.

The experimental discovery and our theory opens a new door. We believe that doped spin-1 Mott insulators are also seats of high T_c superconductivity. This route is worth exploring as there are many spin-1 Mott insulators in nature and more can be synthesized. In what follows we describe our double RVB theory for Fe pnictide systems.

We suggest that LaOFeAs is basically a spin-1 Mott insulator that has become a bad metal by the self-doping of an equal and small density ($y \ll 1$) of electron and hole carriers. External doping in LaOFeAs avoids double exchange ferromagnetism and stabilizes a quantum singlet string liquid (spin-1 Haldane chain [93]). We view the above state as two spin-$\frac{1}{2}$ resonating valence bond (RVB) system, coupled by a weak Hund coupling and bond charge repulsions, leading to an AKLT [94]-type of spin pairing. We write down a model and present an RVB mean field theory. Going beyond mean field theory involving three different projections brings out the string content of the new superconductors. Our estimate of superconducting T_c gives a large value in the range 100 to 200 K. We then briefly indicate how the underlying string structure can bring about real space orders that will in general compete with superconductivity.

The layered transition metal monopnictide $LaOFeAs_{1-x}P_x$ becomes superconducting with a $T_c \approx 5$ K. On replacing P by As, we get LaOFeAs, a bad metal that exhibits a long-range antiferromagnetic (AFM) order below about 125 K but not superconductivity. External doping in LaOFeAs leads to superconductivity with a T_c of 27 K at optimal doping. Various experiments point to a striking similarity to cuprates, even though there is no parent Mott insulator in the present situation. Particularly striking is the phase diagram, T dependence of nuclear spin relaxation and ARPES results that show spin gap behaviour very similar to that in cuprates.

Following the discovery of high T_c superconductivity in LaOFeP and doped LaOFeAs, several groups have performed local density approximations (LDA) and more sophisticated calculations [95–97]. LaOFeAs is a layered material with alternate stacking of LaO and FeAs layers. Fe atoms form a square lattice, a quasi-two-dimensional metal. Each Fe atom is tetrahedrally coordinated by As atoms. Fe^{2+} in LaOFeAs is in $3d^6$ configuration. LDA calculations show five overlapping 3d bands spread in the energy range -2 to $+2$ eV. Individual bands are about 2 eV wide. Filled and empty bands have a small overlap at the Fermi level. LDA calculations present an antiferromagnetic solution with a large moment of about 2 μ_B per Fe atom and also paramagnetic solution. Both solutions have small Fermi
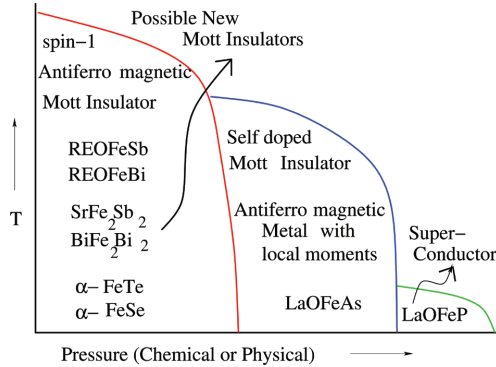
Figure 17. Schematic temperature vs. pressure (chemical or physical) phase diagram. LaOFeAs, a slightly self-doped spin-1 Mott insulator is more correlated than heavily self-doped metallic LaOFeP. Some possible layered spin-1 Mott insulators, with increasing Fe–Fe distance and with a better prospect for higher superconducting T_c are also indicated.

pockets with a Fermi energy of about 0.2 eV. The AFM state has a lower energy of about 87 meV per Fe, compared to paramagnetic solution.

We interpret the existence of a large moment of 2 μ_B per Fe atoms in LDA theory to indicate that Fe^{2+} carries a spin-1 moment in LaOFeAs, the intermediate spin value, rather than the lowest spin-zero or highest value of spin-2. Further, we also take the energy difference between AFM and paramagnetic solution as the effective Hund coupling parameter in the metallic state, $J_H \approx 87$ meV. In order to discuss magnetism or superconductivity originating from a parent Mott insulating state, we have to go beyond LDA theory. It is here that t-J model or Hubbard model has an important role to play. We start our microscopic model here, by taking key inputs from experiments and LDA results about the existence of quantum fluctuating spin-1 moment in Fe ions.

Starting from five bands and reducing it to a spin-1 Mott insulator model is rather difficult. The competing crystal field and covalency effects from four tetrahedral As neighbours and metal–metal bond from four square planar Fe neighbours, Hund coupling and intra- and inter-orbital Hubbard Us makes the problem rather hard. We have taken, as mentioned above, clues from experiments and LDA results in writing down a microscopic effective Hamiltonian.

Chemical or physical pressure converts a Mott insulator into a metal. Long-range Coulomb interaction, which is ignored in the Hubbard model, makes it a first-order transition, as argued by Mott. It was recently suggested by us [5] in the context of organic Mott insulators, that the metallic state in the vicinity of the transition is well described as a self-doped Mott insulator. In the self-doped Mott insulator local moments and superexchange among them survive; however, a small and equal density of electron and hole like carriers (doublon and holon in the context of single orbital spin-$\frac{1}{2}$ Mott insulator) has been created spontaneously and maintained without mutual annihilation, for energetic reasons. Based on the existing phenomenology we suggest the same for LaOFeAs. It is a spin-1 Mott insulator that has a small ($y \ll 1$) density of self-doped carriers.

A consequence of our suggestion is the following prediction, which is summarized in figure 17. Experimentally, Fe–Fe distance increases as we go from LaOFeP to LaOFeAs, because the pnictogen–pnictogen p-bond becomes weaker. If the same trend continues, which is likely, the other two pnictides REOFeSb and REOFeBi and also the chalcogenide FeTe might have a larger Fe–Fe distance, leading to a spin-1 Mott insulating state. In the same vein, LaOFeP has a higher amount of self-doping, and antiferromagnetism gets replaced by superconductivity at low temperatures. Usually hydrostatic pressure has more than one effects, including stiffening of the lattice, buckling of the planes, modifying quantum chemical parameters etc. Some times it is difficult to isolate the effect coming from a change in Fe–Fe distance, that we are focussing on.

Our microscopic Hamiltonian contains two orbitals at the Fermi level. Assuming that the metallic state maintains the square lattice symmetry, there are different possibilities for choosing the symmetry of the two Wannier orbitals: (i) a pair from $3d_{x^2-y^2}$, $3d_{xy}$, $3d_{z^2}$, whose $|\psi|^2$ have square planar symmetry or (ii) $3d_{xz}$ and $3d_{yz}$. As the two planar orbitals $3d_{xy}$ and $3d_{x^2-y^2}$ have strong Fe–Fe metallic bond, cohesive energy will be more if they have a filling close to half. We assume that for LaOFeAs one of the bands has a filling $1 - y$ and the other $1 + y$. For externally doped LaOFeAs, without loss of generality, the fillings are $1 - y$ and $1 + x + y$.

So we choose a simple two-orbital Hamiltonian. Key parameters of our model are the inter- and intra-orbital Hubbard U, ~ 3 to 4 eV, bond charge repulsion $V_{12} \sim$ 1 eV and Hund coupling ~ 0.1 eV. Width of an individual 3d band is about 2 eV, giving a hopping parameter between nearest-neighbour Wannier orbitals, $t \sim 0.5$ eV.

The Hamiltonian of our 2 RVB systems is a two-orbital Hubbard model:

$$H = -\sum_{ij\mu} t_{ij\mu} c_{i\mu\sigma}^\dagger c_{j\mu\sigma} + \text{h.c.} + \sum_{i\mu} U_\mu n_{i\mu\uparrow} n_{i\mu\downarrow}$$

$$+ V_{12} \sum_{\langle ij \rangle} n_{ij1} n_{ij2} - J_{\text{H}} \sum_i \left(\sum_\mu c_{i\mu\alpha}^\dagger \vec{\sigma}_{\alpha\beta} c_{i\mu\beta} \right)^2. \tag{6.1}$$

Here $\mu, \nu = 1, 2$ represent Wannier orbitals. Hopping is assumed to exist only among the same types of nearest-neighbour orbitals. Second line of the above equation (6.1) couples the two systems, through bond charge repulsion and Hund coupling. The operator $n_{ij\mu} \equiv \frac{1}{2} \sum_\sigma (c_{i\mu\sigma}^\dagger + c_{j\mu\sigma}^\dagger)(c_{i\mu\sigma} + c_{j\mu\sigma})$ counts the number of electrons in the bonding state of μth orbital connecting neighbouring sites i and j. The bond charge repulsion is a Coulomb interaction term, $V_{12} = \int |\psi_{i1}(\mathbf{r}) + \psi_{j1}(\mathbf{r})|^2 \frac{e^2}{|\mathbf{r}-\mathbf{r'}|} |\psi_{i2}(\mathbf{r'}) + \psi_{j2}(\mathbf{r'})|^2 \mathrm{d}\mathbf{r}\mathrm{d}\mathbf{r'}$, where $\psi_{i\mu}$ are the two Wannier orbitals at site i. Bond charge repulsion is not usually included in the minimal Hubbard model. In view of its off-diagonal nature in the Wannier basis, this term is sometimes referred to as correlated hopping term. This term provides a local stiffness to a quantum singlet chain string that we will introduce soon. Our mechanism survives even if this term is absent.

Starting from the above Hamiltonian, using a superexchange perturbation theory, we derive the following effective Hamiltonian for the optimally doped case. It is a sum of two t-J models:

$$H_{\text{eff}} \equiv H_{\text{tJ1}} + H_{\text{tJ2}} = -\sum_{ij\mu} t_{ij\mu} c^\dagger_{i\mu\sigma} c_{j\mu\sigma} + \text{h.c.}$$

$$-\sum_{ij} J_{ij\mu} \left(\mathbf{S_{i\mu}} \cdot \mathbf{S_{j\mu}} - \frac{1}{4} n_{i\mu} n_{j\mu} \right) \tag{6.2}$$

with three local constraints: (i) $n_{i\mu\uparrow} + n_{i\mu\downarrow} \neq 0$ or 2, for electron or hole-doped cases, (ii) $\sum_\mu b^\dagger_{ij\mu} b_{ij\mu} \neq 2$ and (iii) $(\sum_\mu c^\dagger_{i\mu\alpha} \vec{\sigma}_{\alpha\beta} c_{i\mu\beta})^2 \neq 0$. Here $b^\dagger_{ij\mu} = \frac{1}{\sqrt{2}}(c^\dagger_{i\mu\uparrow} c^\dagger_{j\mu\downarrow} - c^\dagger_{i\mu\downarrow} c^\dagger_{j\mu\uparrow})$ is the bond singlet operator. The superexchange $J \approx 4t^2/U$. At the Hamiltonian level the 2 RVB systems are decoupled; however the three constraints couple two RVB systems in a nontrivial fashion. The first, double/zero occupancy constraint is well known in t-J model. The second and third are new in the context of superconductivity theory. The second one tells us that two neighbouring sites containing two electrons each cannot form two covalent bonds, because of the bond charge repulsion. The third constraint is dictated by Hund coupling, which favours maximal spin at a given site.

Here we should point out that for doped higher spin Mott insulators (e.g. mangenites) double exchange favours a ferromagnetic metallic state at optimal doping. However for spin-1 case we show below that a spin singlet fluid state is also possible provided the Hund coupling $\frac{1}{4}J_{\text{H}}$ is less than the superexchange coupling J. This is achieved by singlet pairing of the two spin-$\frac{1}{2}$ constituent moments of our spin-1 Fe atoms between neighbours. This is similar in spirit to AKLT spin singlet pairing for the spin-1 chain in one dimension, which leads to a well-known Haldane gap.

We will discuss the above model Hamiltonian, using RVB theory approach [3,23]: (i) solve the unconstrained Hamiltonian in a mean field theory and (ii) perform all projections in the resulting wave function, for further analysis. The unconstrained Hamiltonian is the same as the one solved in the first RVB mean field theory [23] of cuprates. Later, several important improvements [51] have been made on that approach. We can use all those results. Formally the wave function we wish to analyse for superconductivity in our 2 RVB system (for hole density x) is the following:

$$|SC\rangle \approx P_{\text{G}} P_{\text{B}} P_{\text{S}} \left(\sum_{ij} \phi_{ij} b^\dagger_{ij1} \right)^{\frac{N}{2}(1-\frac{x}{2})} \left(\sum_{ij} \phi_{ij} b^\dagger_{ij2} \right)^{\frac{N}{2}(1-\frac{x}{2})} |0\rangle$$

$$\equiv P_{\text{G}} P_{\text{B}} P_{\text{S}} \left(\sum_{ij\mu} \phi_{ij} b^\dagger_{ij1\mu} \right)^{\frac{N}{2}(1-x)} |0\rangle, \tag{6.3}$$

where $b^\dagger_{ij\mu} = \frac{1}{\sqrt{2}}(c^\dagger_{i\mu\uparrow} c^\dagger_{j\mu\downarrow} - c^\dagger_{i\mu\downarrow} c^\dagger_{j\mu\uparrow})$ is the singlet operator. Further, P_{G} is the usual Gutzwiller projection which prevents double occupancy in any of the orbitals. P_{B} avoids two singlet bonds connecting two neighbouring sites. P_{S} projects out the singlet spin component of two electrons at any site. The pair function ϕ_{ij} is the variational wave function. For a single RVB system, in a square lattice, the above function has $d_{x^2-y^2}$ symmetry and leads to a superconducting state with nodal quasi-particles.
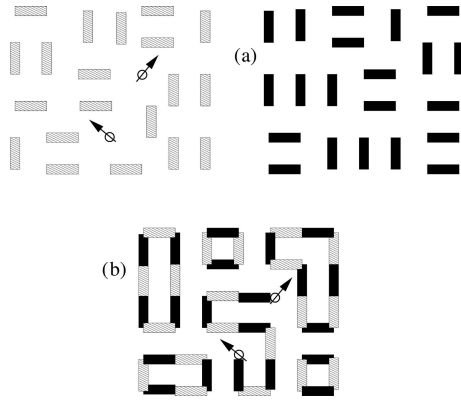
Figure 18. Fusion of valence bond states. (**a**) VB states of the two systems. (**b**) String-like organization after fusion.

In the presence of coupling between two RVB systems, the key questions are: (i) do the three projections preserve d-wave superconductivity of a single RVB system? and (ii) are there going to be some new physics? These are difficult questions to answer. However, the available phenomenology suggests superconductivity, similar to that suggested by 2d repulsive Hubbard model close to half filling survives. In what follows, we will address these questions from the point of view of short-range RVB states and find that projections bring an entirely new quantum liquid, namely quantum string liquid (QSL) and associated rich possibilities.

We also develop a quantum mechanical basis of singlet string states, by an appropriate fusion of two short-range RVB states. We will start with the case of no doping. Consider two nearest-neighbour valence bond (VB) states shown in figure 18. The VBs of two systems are denoted by dark and shaded bonds. If we choose two arbitrary VB states and fuse them, we will get overlapping bonds, in general. Such states are energetically not favourable because of bond charge repulsion energy V_{12}. The two valence bond states in figure 18a do not have bond overlap. When we fuse them we get a state shown in 18b. From simple topological considerations it follows that the resulting state is a set of closed strings. Open strings, if they appear, carry spinons at their ends. Also every configuration of closed and open strings (made of nearest-neighbour bonds) that fill the lattice can be obtained by a fusion of two unique VB states.

Fusion and formation of singlet chain occurs only when we project out singlet states at every site (through the opertator P_S in eq. (6.3)). The bond charge repulsion gives only stiffness to the singlet chain.

Short-range VB states form an overcomplete set of states to describe the physics of a spin-$\frac{1}{2}$ Heisenberg model. The overcompleteness makes different VB states linearly independent and not orthogonal. As our fused states are direct product of two RVB states, we can use known results of single VB overlap properties to study our combined system. It should be remembered that the total number of string states is simply not the square of the number of possible valence bond states, because of the constraints.
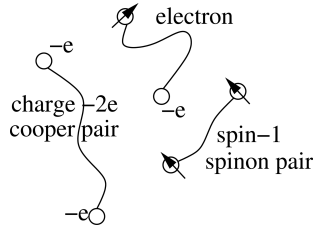
Figure 19. Charge $-2e$ Cooper pair, a spin-1 spinon pair and an electron, as different string states.

Let us calculate the energy expectation value of the bond repulsion and Hund coupling terms in a string state. By construction, bond repulsion energy is zero. Since we have two valence bonds meeting at every site, the total spin value at a given site is fluctuating: with probability $\frac{1}{4}$ it has value zero and with probability $\frac{3}{4}$ it has value 1. Thus, the average value of the Hund coupling energy is $\frac{3}{4}$th of the maximum possible value $2J_H$. It should be pointed out that by going to the double exchange favoured ferromagnetic metallic state we loose a superexchange energy of $2J$. Thus assuming that the kinetic energy gains are identical in both cases, we get a condition $J_H < J$ for the stability of our singlet string liquid phase.

It is possible to gain the extra Hund coupling energy $\frac{1}{4}2J_H$ projecting out the singlet component at every site. Or one can replace every string state formally by the exact ground state of the Haldane gapped nearest-neighbour Heisenberg antiferromagnetic spin-1 chains. Our strings already have an orbital order as the beads alternate along the chain. Converting them into Haldane chains brings an additional topological order [94].

Now we briefly discuss topological excitations in our 2 RVB system. Figure 18b already shows how a two-spinon (spin-1) state appears as an open string. As every unpaired spin or doublon or holon can occur in one of the two orbitals of a given site, they carry an orbital quantm number as well. A bound spinon pair (figure 19) is likely to be a low energy excitation in our metallic system. When we add an electron to the insulating valence bond state, we get a spinon–doublon composite as shown in figure 19. When two electrons are added, it is energetically advantageous to get rid of two unpaired spins. That is, the unpaired spin will disappear as singlets and we will be left with one open string with two doublons (charge $-e$) at the ends (figure 19).

An open string with charges (holon/doublon) at both the ends is our Cooper pair. It is not obvious how it will modify the nature of superconducting state. While the overall off-diagonal long-range order (ODLRO) and phenomenology may resemble the standard Bardeen–Cooper–Schrieffer (BCS) superconductor, there may be subtle topological orders and nontrivial excitations in our quantum string liquid superconductor. It needs to be explored.

String structure suggests, depending on the size of the open string (dictated by factors such as resonance energy, Coulomb repulsion etc.) a binding mechanism for our holon pairs. Is this an additional pairing energy? The final superconducting state will be a coherent superposition of the resonating charge string configurations. A key parameter that determines the superconducting T_c will be the effective mass

of the 2*e* open string. That will give us a Kosterlitz–Thouless-type of scale $k_B T_c \approx \hbar^2 n / 2m_c$, where n is the carrier density per unit area. This expression is very similar to the expression of T_c in RVB theory, suggested by the condensation of charge valence bonds or holons. Thus we expect a maximum T_c in the range of 160 to 200 K, perhaps exceeding cuprates.

Since we have string-like entities, there will be a tendency for them to have liquid crystalline type order, spin order and charge order, encouraged by unscreened long-range interaction at low doping and electron lattice coupling. Such real space organization will in general reduce superconducting T_c. These are competing phases, very much like in cuprates. If one can engineer materials, such as Tl or Hg multi-layer cuprates, where charge and spin order tendencies are suppressed, superconducting T_c's can go higher than 52 K that has been observed so far. Similarly doped LaOFeSb, LaOFeBi, or if they can be synthesized as layered structures, are likely to have higher T_c's.

7. Other routes

Soon after BCS theory, the idea of pairing was applied to nucleons in nuclei, where the scales of energy gaps are very high. One extreme example is superconductivity/superfluidity in neutron stars in the proton/neutron Fermi sea. As the Fermi energy and interaction energy scales in these dense nuclear systems are very high, compared to their terrestrial electron liquid counterparts in solids, the superconducting T_c's can be astronomically high. This gives a feeling that one could find real materials with increased coupling constants and Fermi energies yielding room temperature superconductivity. Unfortunately there are severe constraints posed by quantum chemistry and solid state chemistry. In the theoretical suggestions for new high temperature mechanisms, P W Anderson has been an important critique, from the beginning.

7.1 *Exciton route*

In the simplest form, BCS expression for superconducting T_c is

$$k_B T_c = \hbar \omega_D e^{-1/\lambda \rho_0}. \tag{7.1}$$

Formally, T_c can be increased by increasing the prefactor, the Debye energy and decreasing the argument of the exponential, product of density of states at Fermi level and electron–boson coupling parameter. Little [16], in his original suggestion replaced the Debye energy $\hbar \omega_D$ by an exciton energy of the polarizable side chains of an organic conductor. He estimated various parameters and suggested that one could reach room temperature superconductivity in suitably tailored organic conductors. The commendable aspect of this suggestion, from the point of view of experimental activities, was that it gave rise to the new field of organic conductors. New organic conductors were synthesized, looking for high T_c superconductivity. A parallel development due to Ginzburg [17], envisages a metal–semiconductor–metal sandwich. High energy excitons of the adjacent semiconductor layer was suggested

to mediate pairing leading possibly to room temperature superconductivity. Later, Allander *et al* [98] pursued this idea.

Inkson and Anderson [98] criticized the above ideas and argued that when you go into the actual many-body processes, involving electron–electron interactions (rather than an effective electron–exciton interaction), there is some double counting involved. They argued that in practice there is some subtle cancellations and T_c does not get enhanced. There were interesting exchange between Anderson and Bardeen group. Apart from theory, it is an experimental fact and general consensus that none of the old and new superconductors, including the organic superconductors, follow Little or Ginzburg mechanism.

7.2 *Polaron route*

Anderson [99], in one of his early papers suggested that in some semiconductors, strong electron lattice interaction in certain localized defect centres could overcome Coulomb repulsion, resulting in a net attraction and a stable spin-singlet electron pair states. This suggestion of a negative U Hubbard model was taken by Chakraverty and colleagues [100], who argued for the possibility of high T_c superconductivity. There is again, no experimental proof that this mechanism is at work, in known high T_c superconductors. A major hurdle to this mechanism is that a strongly bound bipolaron formation is also accompanied by band narrowing (Franck–Kondon overlap) and consequent self-trapping of the Cooper pair.

7.3 *Metallic hydrogen route*

Solid hydrogen is expected to become a metal under very high pressure of the order of 100 GPa. At that density, the Debye a frequency is high and it has been suggested that such a metal will exhibit room temperature superconductivity, through the standard electron–phonon mechanism. It has been argued that this should also happen in hydrogen dominant metallic alloys or hydrides [101]. Again, it is an experimental fact that there is no conclusive evidence for high-temperature superconductivity.

8. Some open theoretical problems

Being a fertile and complex field, there are several open theoretical problems in all the five routes that we have suggested in the present article. We will discuss some of them in what follows.

One of the basic problems, common to all the routes, is a rigorous proof for the existence of a superconducting ground state for the t-J model or the repulsive Hubbard model in two-dimensional square lattice for an acceptable range of doping and t, J or U. Traditional approaches using Bogoliubov inequalities are not helpful. I personally believe that within the accepted standards and physical rigor of solid state physics, RVB theory has proved the existence of high-temperature

superconductivity in the t-J model. Further, a variety of approximate analytical and numerical methods have been developed to calculate the physical quantities. However, a more precise mathematical proof will remove the trace of doubt that stays in the minds of the community. Elsewhere I have drawn an analogy [102] of the current situation in the theory of high T_c superconductivity to the problem of proving quark confinement in the $SU(3)$ gauge theory of strong interaction, in the field of elementary particle physics. There are good proofs for confinement, within the acceptable rigor and standards of particle physics phenomenology. There are also methods such as lattice gauge theory, perturbative QCD and some nonperturbative methods to compute physical quantities. However, there is no rigorous proof for confinement. Clay Mathematics Institute has declared proving the presence of a finite mass gap in Yang–Mills theory, which is equivalent to proving colour confinement, as a millenium problem.

I have stressed elsewhere [35,52] that a large variation of T_c among the many family members of cuprates is due to some underlying physics related to other completing orders, sometimes encouraged by phonons, rather than a simple quantum chemical change of the parameters t, t' and t''. It will be nice to investigate this theoretically, for example, in variational Monte Carlo approaches by including, phonon degrees of freedom.

In the pressure route, we need to do quantitative estimate of the self-doping density for various organics, using a semi-phenomenological approach incorporating long-range Coulomb interaction. Such an analysis will help one pinpoint the underlying physics that controls the amount of self-doping. From experimental point of view we need to optimize the self-doping density to maximize T_c.

In the diamond route, even though we have provided a scenario and ways of estimating T_c, a many-body theory analysis, even at the level of variational Monte Carlo analysis does not exist. It will be nice to perform these calculations for these 'dirty RVB superconductors'. There might be some surprise arising from disorder.

Graphene route is at the very beginning. Variational wave functions and analysis going beyond what we have done in ref. [7] will be welcome. As for the iron route, again we are at the beginning. The only calculation that exists in the RVB approach is our result, where we have reduced the 2-RVB system essentially to a single RVB system. Going beyond this will be valuable, as the 2 RVB system has a more complex structure and consequently richer physics.

9. Conclusion

It is indeed interesting that in spite of important developments from electron correlation-based mechanism of high T_c superconductivity, there has not been serious attempts to suggest new routes for high T_c superconductivity within this mechanism. A notable exception is a suggestion from Kivelson and collaborators [103], who suggested that quasi-one-dimensional inhomogeneities such as fluctuating or static stripe play an important role in stabilizing high T_c superconductivity. The basic idea is that such inhomogeneities (low-dimensional structures) allow development of strong pairing correlations from electron repulsion mechanism. In order to make use of such a well-developed pairing correlation in developing superconductivity in the plane, electron pair tunnelling between the stripes is invoked. In our

opinion, this attractive suggestion suffers from some serious criticism, at least from the example of cuprates: (i) in the optimally doped regime, where T_c is maximum, the system is homogeneous at low energy scales and there is no tendency for charge localization into lower-dimensional structures and (ii) such low-dimensional structures or charge localization is accompanied by reduction in T_c (on the under-doped side for example). Thus, it is not clear if fluctuating lower-dimensional structures are helpful to enhance T_c. Indeed they inhibit T_c by being competitors at least in layered systems.

As we have already explained, the copper route remains largely unexplored. A systematic effort to dope spin-$\frac{1}{2}$ Mott insulators, that pass various hurdles, is needed. Nonequilibrium methods for forceful doping need to be developed.

Pressure route has been extremely useful in showing some matters of principle: for example, an often made statement is that 'everything will superconduct under suitable pressure'. That seems to be happening. Even Fe becomes superconducting under pressure. On the other hand, the pressure we are talking about is within the regime of Mott insulators without destroying the integrity of the underlying Mott state significantly. Organic superconductors are excellent guide. It will be wonderful to metallize one of the Mott insulating cuprates La_2CuO_4 and CuO. One success will make this an attractive direction.

In the diamond route, there seems to be as many possibilities as there are band insulators. The choice of dopants with the right quantum chemistry is a key aspect. A major problem is how to dope them to the desired extent without changing the integrity of the band insulator. The possibility of nitrogen doping in diamond is an example which illustrates the difficulties rather well.

In the graphene route we have theoretically suggested room temperature superconductivity in graphene at an optimal doping. This should be tried.

The last, double RVB or iron route is very fascinating. We did not expect a spin-1 Mott insulator to become superconducting on doping. But nature seems to be showing a way along this line in the new Fe pnictide superconductors.

References

[1] A Bednorz and A Muller, *Z. Phys.* **B64**, 189 (1986)
[2] M Cohen and P W Anderson, in: *Superconductivity in d- and f-band metals* edited by D H Douglass (AIP, New York, 1972) p. 17
[3] P W Anderson, *Science* **235**, 1196 (1987)
[4] K H Hock, H Nickisch and H Thomas, *Helv. Phys. Acta* **56**, 237 (1983)
[5] G Baskaran, *Phys. Rev. Lett.* **90**, 197007 (2003)
    F C Zhang, *Phys. Rev. Lett.* **90**, 207002 (2003)
    G Baskaran and E Tosatti, *Curr. Sci.* **61**, 33 (1991)
    G Baskaran, *J. Phys. Chem. Solids* **56**, 1957 (1995); *Physica* **B223–224**, 490 (1996); *Phys. Rev. Lett.* **91**, 097003 (2003)
[6] G Baskaran, *J. Supcond. Nov. Magnetism* **21**, 45 (2008); *Sci. Technol. Adv. Mater.* **7**, S49 (2006); *Sci. Technol. Adv. Mater.* **9**, 044104 (2008)
[7] S Pathak, V Shenoy and G, Baskaran, arXiv:0809.0244
[8] G Baskaran, *J. Phys. Soc. Jpn.* **77**, 113713 (2008)
[9] D Jerome, *Science* **252**, 1509 (1991)

C Bourbonnais and D Jerome, in: *Advances in synthetic metals* edited by B Bernier *et al* (Elsevier, 1999) p. 206

T Vuletic *et al*, *E. Phys. J.* **B25**, 319 (2002)

[10] T Ishiguro *et al*, *Organic superconductor* (Springer, Berlin, 1998)

[11] E A Ekimov *et al*, *Nature (London)* **428**, 542 (2004)

[12] E Bustarret *et al*, *Phys. Rev. Lett.* **93**, 237005 (2004)

[13] Y Takano *et al*, *Appl. Phys. Lett.* **85**, 2852 (2004)

[14] Y Kamihara, *J. Am. Chem. Soc.* **128**, 10012 (2006)

[15] Y Kamihara *et al*, *J. Am. Chem. Soc.* **130**, 3296 (2008)

[16] W A Little, *Phys. Rev.* **134**, A1416 (1964)

[17] V L Ginzburg, *Sov. Phys. Usp.* **13**, 335 (1970)

[18] L Pauling, *Nature of the chemical bond* (Cornell University Press, NY, 1960)

[19] P W Anderson, *Mater. Res. Bull.* **30**, 1108 (1971)

[20] E H Lieb and F Y Wu, *Phys. Rev. Lett.* **20**, 1445 (1968)

[21] S A Kivelson, D Rokhsar and J Sethna, *Phys. Rev.* **B38**, 8865 (1987)

[22] S Liang, B Doucot and P W Anderson, *Phys. Rev. Lett.* **61**, 365 (1988)

T Hsu, *Phys. Rev.* **B41**, 11379 (1990)

[23] G Baskaran, Z Zou and P W Anderson, *Solid State Commun.* **63**, 973 (1987)

[24] A Kitaev, *Ann. Phys.* **303**, 2 (2003)

[25] G Baskaran and R Shankar (in preparation)

[26] G Baskaran, *Phys. Rev.* **B64**, 092508 (2001)

[27] G Baskaran and P W Anderson, *Phys. Rev.* **B37**, 580 (1988)

[28] I Affleck *et al*, *Phys. Rev.* **B38**, 745 (1988)

[29] I Affleck and J B Marston, *Phys. Rev.* **B37**, 3774 (1988)

[30] G Kotliar, *Phys. Rev.* **B37**, 3664 (1988)

[31] C Gros, R Joynt and T M Rice, *Z. Phys.* **B68**, 425 (1987)

[32] F C Zhang and T M Rice, *Phys. Rev.* **B37**, 3759 (1988)

[33] P W Anderson, G Baskaran, Z Zou and T Hsu, *Phys. Rev. Lett.* **58**, 2790 (1987)

[34] G Baskaran, *Mod. Phys. Lett.* **B14**, 377 (2000)

[35] G Baskaran, *Phys. Rev. Lett.* **91**, 097003 (2003)

[36] P W Anderson and G Baskaran (unpublished 1987)

[37] A Ramirez, *Superconductivity Rev.* **1**, 1 (1994)

[38] O Zhou *et al*, *Phys. Rev.* **B52**, 483 (1995)

[39] H Schulz *et al*, *J. Physique-Lett.* **279**, L-51 (1981)

L N Bulaevski, *Adv. Phys.* **37**, 443 (1988)

T Gimamarchi, *Physica* **B230–232**, 975 (1997)

[40] H Kino and H Fukuyama, *J. Phys. Soc. Jpn* **64**, 2726 (1995)

[41] M M Abd-Elmeguid *et al*, *Phys. Rev. Lett.* **93**, 126403 (2004)

[42] M Capone *et al*, *Science* **296**, 2364 (2002)

[43] N F Mott, *Phil. Mag.* **6**, 287 (1961)

[44] V Vescoli *et al*, *Science* **281**, 1181 (1998)

L Degiorgi (private communication)

[45] B N Brockhouse, *Phys. Rev.* **54**, 781 (1954)

X G Zheng *et al*, *Phys. Rev. Lett.* **85**, 5170 (2000)

[46] I Loa *et al*, *Phys. Rev. Lett.* **87**, 125501 (2001)

[47] J P Locquet, *Nature (London)* **394**, 453 (1998)

[48] The author thank 'http://www.sxc.hu/home' for making the blue diamond picture available for our use

[49] M Milovanovic, S Sachdev and R N Bhatt, *Phys. Rev. Lett.* **63**, 82 (1989); **48**, 597 (1982)

M A Paalanen *et al*, *Phys. Rev. Lett.* **61**, 597 (1988)

M Lakner *et al*, *Phys. Rev.* **50**, 17064 (1994)

[50] R N Bhatt and T M Rice, *Phys. Rev.* **B23**, 1920 (1981)

R N Bhatt and P A Lee, *Phys. Rev. Lett.* **48**, 344 (1982)

[51] P W Anderson *et al*, *J. Phys.: Condense Matter* **24**, R755 (2004)

[52] G Baskaran, *Iran. J. Phys. Res.* **6**, 163 (2006)

[53] B Sacepe *et al*, *Phys. Rev. Lett.* **96**, 097006 (2006)

[54] A Therese Pushpam and T Navaneethakrishnan, *Solid State Commun.* **144**, 153 (2007)

[55] Erik Nielsen and R N Bhatt, arXiv:0705.2038

[56] Superconducting 'dome' was theoretically predicted first in the paper, P W Anderson *et al*, *Phys. Rev. Lett.* **58**, 2790 (1987)

[57] E Bustarret *et al*, *Nature (London)* **444**, 465 (2006)

[58] Z A Ren *et al*, *J. Phys. Soc. Jpn* **76**, 103710 (2007)

[59] T Shirakawa, S Horiuchi and H Fukuyama, *J. Phys. Soc. Jpn* **76**, 014711 (2007)

[60] E A Ekimov *et al*, *Sci. Technol. Adv. Mater.* **9**, 044210 (2008)

N Dubrovinskaia *et al*, *Appl. Phys. Lett.* **92**, 132506 (2008)

[61] D S Fisher *et al*, *Phys. Rev. Lett.* **61**, 482 (1988)

[62] G Baskaran, unpublished

[63] M Alaeia, S Akbar Jafari and H Akbarzadeha, arXiv:0807.4882 (to appear in *J. Phys. Chem. Solids*)

[64] T Venkatesan, National University of Singapore, Project on 'Superhydrogenic State Superconductivity'

[65] J Nagamatsu *et al*, *Nature (London)* **410**, 63 (2001)

[66] A K Geim and K S Novoselov, *Nat. Mater.* **6**, 183 (2007)

[67] M I Katsnelson, *Mater. Today* **10**, 20 (2007)

[68] A H Castro Neto *et al*, arXiv.org:0709.1163 (2008)

[69] G Baskaran, *Phys. Rev.* **B65**, 212505 (2002)

[70] A M Black-Schaffer and S Doniach, *Phys. Rev.* **B75**, 134512 (2007)

[71] B Uchoa and A H Castro Neto, *Phys. Rev. Lett.* **98**, 146801 (2007)

[72] T C Choy and B A McKinnon, *Phys. Rev.* **B52**, 14539 (1995)

[73] N Furukawa, *J. Phys. Soc. Jpn* **70**, 1483 (2001)

[74] S Onari *et al*, *Phys. Rev.* **68**, 024525 (2003)

[75] D Baeriswyl and E Jackelman, in: *The Hubbard model: Its physics and mathematical physics* edited by D Baeriswyl (Plenum, New York, 1995) p. 393

[76] G Baskaran and S A Jafari, *Phys. Rev. Lett.* **89**, 016402 (2002)

[77] D Ceperley, G Chester and M Kalos, *Phys. Rev.* **65**, 1032 (1977)

[78] M C Gutzwiller, *Phys. Rev.* **137**, A1726 (1965)

[79] H Shiba, in: *Two-dimensional strongly correlated electron systems* edited by Zi-zhao Gan and Zhao-bin Su (Gordon and Breach Science Publishers, 1989)

[80] A Paramekanti, M Randeria and N Trivedi, *Phys. Rev.* **70**, 054504 (2004)

[81] S Florens and A Georges, *Phys. Rev.* **70**, 035114 (2004)

[82] E Zhou and A Paramekanti, *Phys. Rev.* **76**, 195101 (2007)

[83] C Honerkamp, *Phys. Rev. Lett.* **100**, 146404 (2008)

[84] T M Klapwijk, *Nat. Phys.* **1**, 17 (2005)

[85] T E Weller *et al*, *Nat. Phys.* **1**, 39 (2005)

[86] R R da-Silva, J H S Torres and Y Kopelevich, *Phys. Rev. Lett.* **87**, 147001 (2001)

[87] Y Kopelevich and P Esquinazi, *J. Low Temp. Phys.* **146**, 5 (2007)

[88] S Lebedev, arXiv:0802.4197 (2008)

[89] Y Jiang *et al*, *Phys. Rev.* **B77**, 235420 (2008)

G Baskaran

[90] Hai-Hu Wen *et al*, cond-mat/0803.3021
[91] Z A Ren *et al*, cond-mat/0803.4234
     G F Chen *et al*, cond-mat/0803.4384
[92] Z A Ren *et al*, cond-mat/0803.4283
[93] F D M Haldane, *Phys. Rev. Lett.* **50**, 1153 (1983)
[94] I Affleck *et al*, *Phys. Rev. Lett.* **59**, 799 (1987)
     M den Nijs and K Rommelse, *Phys. Rev.* **40**, 4709 (1989)
     S M Girvin and D P Arovas, *Phys. Scr.* **T27**, 156 (1989)
[95] S Lebegue, *Phys. Rev.* **B75**, 035110 (2007)
[96] D J Singh and M-H Du, cond-mat/0803.0429
     K Haule *et al*, cond-mat/0803.1279
     G Xu *et al*, cond-mat/0803.1282
     Chao Cao *et al*, cond-mat/0803.3236
     Hai-Jun Zhang *et al*, cond-mat/0803.4487
     L Boeri *et al*, cond-mat/0803.2703
     Gang Xu *et al*, cond-mat/0803.1282
[97] K Kuroki, cond-mat/0803.3325
     Xi Dai *et al*, cond-mat/0803.3982
     I I Mazin *et al*, cond-mat/0803.2740
     F Marsiglio and J E Hirsch, cond-mat/0804.0002
     Tao Li, cond-mat/0804.0536
     G Giovannetti *et al*, cond-mat/0804.0866
     S Raghu *et al*, cond-mat/0804.1113
[98] J C Inkson and P W Anderson, *Phys. Rev.* **B8**, 4429 (1973)
     D Allender, J Bray and J Bardeen, *Phys. Rev.* **B8**, 4433 (1973)
     D Allender, J Bray and J Bardeen, *Phys. Rev.* **B7**, 1020 (1973)
[99] P W Anderson, *Phys. Rev. Lett.* **34**, 953 (1975)
[100] B K Chakraverty and C Schlenker, *J. Phys. (Paris) Colloq.* **37**, C4-353 (1976)
      A Alexandrov and J Ranninger, *Phys. Rev.* **B23**, 1796 (1981)
[101] N W Ashcroft, *Phys. Rev. Lett.* **92**, 187002 (2004)
[102] G Baskaran, *Phys. Canada* **56**, 236 (2000)
[103] S Kivelson, *Physica* **B318**, 61 (2002)